Kokkedee, J. J. J.
1962

Physica 28
374–408

ANHARMONIC EFFECTS IN THE COHERENT SCATTERING OF NEUTRONS BY CRYSTALS

A FORMAL TREATMENT OF SHIFT AND WIDTH OF THE PEAKS IN THE SCATTERING SPECTRUM

by J. J. J. KOKKEDEE

Instituut voor theoretische fysica der Rijksuniversiteit, Utrecht, Nederland.

Synopsis

As predicted by harmonic theory the outgoing inelastic spectrum of neutrons, scattered coherently by a single crystal, for a particular angle of scattering consists of a number of delta-function peaks superposed on a continuous background. The peaks correspond to one-phonon processes in which one phonon is absorbed or emitted by the neutron; the background corresponds to multi-phonon processes. When anharmonic forces are present the delta-function peaks are broadened into finite peaks and are shifted relative to those predicted in the harmonic approximation. These anharmonic effects are treated by means of many particle perturbation theory, in which the anharmonic part of the Hamiltonian is considered as the perturbation (phonon-phonon interaction). Use has been made of diagrams for representing the various matrix elements. Since the one-phonon peaks are considered as separate from the background without confining oneself to lowest order perturbation theory, the treatment is restricted to the case where the line width of a phonon state is small with respect to the energy of the phonon also for strong coupling between the phonons. In this connection the results obtained are expected to be valid only in the temperature range from absolute zero up to temperatures not much higher than the Debye temperature. For these temperatures the influence of two-phonon processes on the line shape may be neglected. An expansion for calculating the line shift and line width in powers of u/d and in terms of simple connected diagrams is obtained (u is the average atomic displacement, d is the smallest interatomic distance in the crystal). Formulae, which express the shift and width in the parameters of the lattice, are given valid to order $(u/d)^2$.

1. *Introduction.* Up to now practically all theoretical work that has been done in the field of scattering of thermal neutrons by crystals has been based on the assumption that the crystal may be treated in the harmonic approximation, that is after expanding the potential energy term in the Hamiltonian of the crystal in powers of the atomic displacements only terms through second order are retained[1]). In general this assumption is justified for temperatures far below the melting point for those situations where one is only interested in the intensity of the scattering (total cross

sections and the like). However, in the detailed structure of the coherent inelastic spectrum*) anharmonic forces show up in a very interesting way, giving rise to appreciable effects even at absolute zero.

When energy is exchanged between the neutron and the crystal the scattering is called inelastic. For a particular angle of scattering the coherent inelastic spectrum, predicted by harmonic theory, consists of a number of pure lines or delta-function peaks over a continuous background[2]). The peaks correspond to the so-called one-phonon processes in which the neutron excites or de-excites a single phonon in passing through the crystal; the locations of the peaks follow from the conservation rules for energy and momentum. The one-phonon peaks, and therefore the one-phonon processes are particularly interesting from the point of view of crystal dynamics. The background of the inelastic spectrum is produced by the multi-phonon processes in which the neutron excites or de-excites more than one phonon per single scattering event. The multi-phonon processes are expected not to give rise to peaks in the scattering spectrum, however, with the exception of the two-phonon processes. Under certain circumstances, as has been proved by Sjölander[3]), these processes can cause logarithmic singularities centered on the delta-function peaks. Multi-phonon processes become important for temperatures well above the Debye temperature or for energies of the incoming neutron which are large in comparison to $k_B T_D$ (k_B is Boltzmann's constant, T_D is the Debye temperature of the crystal).

When anharmonic forces are present they will manifest in a most significant way in the above mentioned one-phonon peaks. Anharmonic forces, if small, can be interpreted as causing an interaction between phonons; as a result of this phonon-phonon interaction the phonons get a finite lifetime while the energies are shifted with respect to the undisturbed values (self-energy effects), the undisturbed values being the values calculated for a harmonic lattice with parameters adjusted at the temperature under consideration, thus including the effects of thermal expansion at that temperature. As a consequence the inelastic spectrum now exhibits finite peaks rather than delta-function singularities, which are shifted relative to those predicted in the harmonic approximation at the temperature under consideration. The effects of energy shift and width will be functions of temperature.

Recent experiments of Brockhouse a.o.[4]) on lead and of Larsson a.o.[5]) on aluminium have demonstrated the abovementioned anharmonic effects. In both cases line widths are found which increase almost linearly with temperature, the temperature range covering the region from the neighbour-

*) We restrict ourselves to a discussion of the coherent inelastic scattering, because in this case the anharmonic forces give rise to much more interesting features than in the case of incoherent scattering and elastic coherent scattering (see § 5). Furthermore we only consider scattering by single crystals.

hood of the Debye temperature (~90°K for lead and ~375°K for aluminium) to the neighbourhood of the melting point. In the lower part of this region up to temperatures equal to two or three times the Debye temperature the measured line widths are relatively small corresponding to phonon lifetimes which are several times larger than a vibrational period. For much higher temperatures values of the width are found that are much larger, corresponding to phonon lifetimes of the order of a vibrational period. Furthermore Larsson finds a frequency shift of the peaks to lower values with increasing temperature, the total variation being 15% over the temperature range $300° \leqq T \leqq 932°K$.

Brockhouse a.o.[4]) try to explain their experimental results in a phenomenological way by adding to the Born- von Kármán equations of motion of the crystal dissipative terms proportional to the relative velocities of the ions, these terms giving rise to a finite phonon lifetime. In general ,however, such simple theories are complicated in the phonon case by the different polarizations of the phonons. Moreover they can only be expected to give reliable results in so far as the line shift and line broadening effects are independent of each other.

Recently Baym[6]) has given a formal treatment of the neutron scattering problem including anharmonic forces by using thermodynamic Green's function methods. However, he does not explicitly treat the effects we are interested in.

Our aim is to study the effects of line shift and line broadening of the peaks of the inelastic scattering spectrum by means of many particle perturbation theory. Such an undertaking has already been started by Van Hove[7]) for the relatively simple case of the crystal in its ground state ($T = 0°K$). Treating the one-phonon peaks as separate from the background, he finds by means of time-independent perturbation methods, developed by Hugenholtz and himself[7])[8]), which are based on the resolvent operator, an expansion of line width and line shift in powers of u/d, where u is an average atomic displacement and d is the smallest equilibrium distance between two atoms in the crystal.

We shall extend Van Hove's approach to the more general case of non-zero temperatures. For this purpose time dependent perturbation theory is more suited than the resolvent methods. However, since we do not want to give a treatment which is limited to lowest order perturbation theory and still want to treat the scattering peaks as separate from the background, we shall restrict ourselves to the case where the line width of a phonon state is small with respect to the energy of the phonon not only in the limit of vanishing coupling between the phonons, but also for actual, i.e. finite values of the coupling constant. Or in other words the uncertainty in the energy of a phonon should be much smaller than the energy itself, also in the case of strong coupling. Only if this condition is satisfied, we can

consider one-phonon peaks as being well defined to higher order in the coupling. The same condition has been formulated by Nosanow[9]) in a general way as being necessary for the construction of metastable states in strongly coupled systems. It is reasonable to expect that this assumption is correct for a temperature range, extending from absolute zero till temperatures not too far above the Debye temperature for any particular crystal. The experiments of Brockhouse and Larsson, mentioned above, seem to support this expectation, although experimental results for lower temperatures, below the Debye temperature, are not available. For the higher temperatures where the phonon lifetime becomes of the order of a vibrational period our assumption is certainly not valid.

In the lower temperature region and for incoming neutron energies small compared to $k_B T_D$, it is furthermore a good approximation to neglect the effects of the two-phonon processes *) on the line shape of the peaks of the scattering spectrum, the one-phonon processes being dominant at these temperatures[1]).

In conclusion we may say that our study applies only to temperatures not much larger than the Debye temperature. There is a good hope that for these temperatures the condition $\Gamma(\boldsymbol{q})/\omega_{\boldsymbol{q}} \ll 1$ is satisfied ($\Gamma(\boldsymbol{q})$ is an average value for the inverse lifetime of the phonon with wave vector $\boldsymbol{q}$ and frequency $\omega_{\boldsymbol{q}}$); the validity of this condition can only be decided by experiment. If this condition is not fulfilled the scattering peaks are not distinguishable from the background. For the high temperature case, high with respect to the Debye temperature, time dependent perturbation theory can also be applied to construct a more general theory. Such a theory must include two-phonon processes and it must avoid the simplifying assumption ($\Gamma(\boldsymbol{q})/\omega_{\boldsymbol{q}} \ll 1$) used in our work.

In the case of metals there is in addition to the phonon-phonon interaction a strong coupling between the phonons and the conduction electrons, which affects the lifetime of the phonon. For temperatures low compared to the Debye temperature the effects of electron-phonon interaction on the scattering spectrum are expected to become considerable. However, we only mention the problem; we shall not be concerned with it here.

In § 2 we present a short survey of the quantum theory of the vibrating

*) It is noteworthy, that in speaking of one-phonon processes, two-phonon processes, etc. we must bear in mind that in the case of scattering by an anharmonic crystal these notions have not such definite meaning as for a harmonic crystal, in the sense that to general order in the phonon-phonon coupling it is in principle not possible (without additional assumptions [6])) to write the inelastic scattering function as a series in which the n-th term just describes the n-phonon processes (phonon expansion). There is a mixing up of the various processes; only the total inelastic scattering function has a physical meaning. From this it follows that, although the scattering peaks, if sufficiently narrow, can be considered as separate from the background in the sense that they are sharply distinguishable from the background and possess well defined locations and widths, one can never make an exact, physically meaningful distinction between peaks and background, however small the (finite) widths of the peaks.

anharmonic crystal, taken as a many body system of interacting phonons. Then in § 3 the differential scattering cross section for the coherent scattering of slow neutrons by crystals will be written in a form, suited for a perturbation analysis. We shall make extensive use of diagrams for representing the relevant matrix elements. The description of these diagrams together with some of their properties will form the contents of § 4. The following four sections will contain the main part of the work. In § 5 and § 6 we define the diagrams which describe the peaks in the inelastic spectrum, and investigate their general structure. The summation of these diagrams will be performed in §§ 7 and 8 by extending a method of Beliaev [14]) to the case of non zero temperatures. In section 8 we give an expression for the partial scattering function describing the peaks, valid to all orders in the interaction but to first order in the parameter $\Gamma(\boldsymbol{q})/\omega_{\boldsymbol{q}}$, which explicitly contains the anharmonic effects we are interested in. Formulae for the line shift and line width, valid to lowest order in the interaction, will be derived in § 9, which express these quantities in the parameters of the lattice at temperature T. Finally the last section is devoted to some remarks concerning a possible quantitative calculation of the effects studied in this paper*).

2. *The anharmonic crystal as a perturbation problem***). We consider a finite, perfect crystal of volume Ω with periodic boundary conditions, containing N_0 unit cells. The rigid-lattice equilibrium positions of all the atoms in the crystal will be designated by vectors $\boldsymbol{R}_{sn}$, which are given by

$$\boldsymbol{R}_{sn} = \boldsymbol{s} + \boldsymbol{R}_{0n}. \tag{2.1}$$

Here $\boldsymbol{s}$ is a crystal translation vector, which can be written as an integral linear combination of three primitive translation vectors $\boldsymbol{d}_1$, $\boldsymbol{d}_2$ and $\boldsymbol{d}_3$:

$$\boldsymbol{s} = s_1\boldsymbol{d}_1 + s_2\boldsymbol{d}_2 + s_3\boldsymbol{d}_3, \tag{2.2}$$

where s_1, s_2 and s_3 are positive or negative integers or zero. The vector $\boldsymbol{R}_{0n}$ gives the position of atom n in the unit cell on the origin, n running from 1 to n_0, the number of atoms per unit cell. In a vibrating crystal the actual position $\boldsymbol{r}_{sn}$ of an atom will be given by the sum of its rigid-lattice equilibrium position and a displacement vector $\boldsymbol{u}_{sn}$, as follows

$$\boldsymbol{r}_{sn} = \boldsymbol{R}_{sn} + \boldsymbol{u}_{sn}. \tag{2.3}$$

Adopting the Born-Oppenheimer approximation for the vibrating crystal we can write the Hamiltonian of the crystal as a sum of two parts: the

*) During the correction of the manuscript the paper of Kashcheev and Krivoglaz [16]) appeared. These authors study the same effects as done here, using Green's function methods; however, their treatment is restricted to lowest order perturbation theory. To this order their results agree with ours.

**) In this section and the following one we closely follow the formulation and notation of L. Van Hove [7]).

kinetic energy of the atoms and a potential energy term. It is usual to expand the potential energy in powers of displacements of the atoms from their equilibrium positions. The resulting Hamiltonian can be written in the form:

$$H = H^{(2)} + V. \tag{2.4}$$

$H^{(2)}$ is called the harmonic energy; it includes all the terms through second order in products of the displacements. V, the anharmonic energy, includes all terms of higher order.

When anharmonic forces are present the equilibrium positions of the atoms do not correspond to those predicted by rigid-lattice theory, not even at absolute zero due to the zero point energy. The equilibrium positions and therefore the atomic force constants of an anharmonic crystal change with temperature. In actual calculations we must carefully treat these effects (see § 10).

The harmonic energy $H^{(2)}$ can be written as follows:

$$H^{(2)} = \varepsilon_0 + \tfrac{1}{2} \sum_{sn} m_n |\dot{\boldsymbol{u}}_{sn}|^2 + V^{(2)}, \tag{2.5}$$

where

$$V^{(2)} = \sum_{ss'} \sum_{nn'} \sum_{\alpha\alpha'} C^{(2)}_{s-s',nn',\alpha\alpha'} u_{sn\alpha} u_{s'n'\alpha'}. \tag{2.6}$$

In these equations ε_0 is the equilibrium rigid-lattice energy of the crystal, m_n the mass of a nucleus of type n and $u_{sn\alpha}$ denotes the α'th rectangular component of the vector $\boldsymbol{u}_{sn}$.

The anharmonic energy V is given by the following equation:

$$V = \sum_{\nu=3}^{\infty} V^{(\nu)}, \tag{2.7}$$

where

$$V^{(\nu)} = \sum_{s_1 \ldots s_\nu} \sum_{n_1 \ldots n_\nu} \sum_{\alpha_1 \ldots \alpha_\nu} C^{(\nu)}_{s_1 n_1 \alpha_1 \ldots s_\nu n_\nu \alpha_\nu} u_{s_1 n_1 \alpha_1} \cdots u_{s_\nu n_\nu \alpha_\nu}. \tag{2.8}$$

The coefficients $C^{(\nu)}_{s_1 n_1 \alpha_1 \ldots s_\nu n_\nu \alpha_\nu}$ (including $\nu = 2$) are proportional to a ν'th order derivative of the rigid-lattice energy, evaluated for the equilibrium lattice. The second order coefficients $C^{(2)}_{s-s',nn',\alpha\alpha'}$ only depend on $\boldsymbol{s}$ en $\boldsymbol{s}'$ through the separation vector $\boldsymbol{s} - \boldsymbol{s}'$.

The expectation value of the ν'th order term $V^{(\nu)}$ in equation (2.7) is of the order of magnitude $\omega(u/d)^{\nu-2}$ ($\nu = 2, 3, \ldots$), ω being a characteristic atomic vibration frequency, u being an average atomic displacement for a given temperature and d being the smallest equilibrium distance between two nuclei. At temperatures which are low compared to the melting point u/d is much smaller than 1. The terms $V^{(\nu)}$ then decrease rapidly with increasing ν and V itself can be considered as a small term in the Hamiltonian H. Under these circumstances we may treat the effects of anharmonic forces on crystal vibration phenomena by means of perturbation methods, the relative strength of the perturbation potential being measured by the parameter u/d.

The solution of the harmonic problem, in which V in equation (2.4) is set equal to zero, gives a description of the vibrating crystal in terms of independent phonons. Each phonon is characterized by a wave vector $\boldsymbol{q}$ and a polarization index j, the vector $\boldsymbol{q}$ being defined up to the addition of 2π times a vector of the reciprocal lattice. For a crystal with an equal number of unit cells along each of the three directions of the primitive translation vectors $\boldsymbol{d}_1$, $\boldsymbol{d}_2$ and $\boldsymbol{d}_3$ and with periodic boundary conditions, $\boldsymbol{q}$ is given by

$$\boldsymbol{q} = 2\pi N_0^{-1/3}\boldsymbol{\tau}, \tag{2.9}$$

where $\boldsymbol{\tau}$ is a vector of the reciprocal lattice; the vector $\boldsymbol{q}$ is restricted to the first Brillouin zone. The polarization index j runs over all positive integers from 1 to $3n_0$. The energy of the phonon $\boldsymbol{q}j$ will be denoted by $\omega_{\boldsymbol{q}j}$(we set $\hbar$ equal to 1). The functions $\omega_{\boldsymbol{q}j}$ are periodic in $\boldsymbol{q}$-space with period $2\pi\boldsymbol{\tau}$. They remain unchanged when $\boldsymbol{q}$ is replaced by $-\boldsymbol{q}$.

The displacement vector $\boldsymbol{u}_{sn}$ of the atom of type n can be expressed in the creation and annihilation operators $a^*_{\boldsymbol{q}j}$ and $a_{\boldsymbol{q}j}$ of the phonon $\boldsymbol{q}j$:

$$\boldsymbol{u}_{sn} = \Sigma_{\boldsymbol{q}} \Sigma_j (2m_n N_0 \omega_{\boldsymbol{q}j})^{-\frac{1}{2}} (a_{\boldsymbol{q}j} + a^*_{-\boldsymbol{q}j})(\boldsymbol{e}^{(n)}_{\boldsymbol{q}j} - i\boldsymbol{f}^{(n)}_{\boldsymbol{q}j}) \exp[i\boldsymbol{q}\cdot\boldsymbol{s}]. \tag{2.10}$$

Here the real vectors $\boldsymbol{e}^{(n)}_{\boldsymbol{q}j}$ and $\boldsymbol{f}^{(n)}_{\boldsymbol{q}j}$ determine the polarization of the phonon $\boldsymbol{q}j$. They are periodic functions in $\boldsymbol{q}$-space with periods $2\pi\boldsymbol{\tau}$ and they are symmetric and anti-symmetric respectively on inversion of $\boldsymbol{q}$. The summation over $\boldsymbol{q}$ is restricted to the first Brillouin zone.

The operators $a_{\boldsymbol{q}j}$ and $a^*_{\boldsymbol{q}j}$ satisfy the following commutation rules:

$$[a_{\boldsymbol{q}j}, a^*_{\boldsymbol{q}'j'}] = \delta_{jj'}\Delta_{\boldsymbol{q}-\boldsymbol{q}'}; [a_{\boldsymbol{q}j}, a_{\boldsymbol{q}'j'}] = [a^*_{\boldsymbol{q}j}, a^*_{\boldsymbol{q}'j'}] = 0. \tag{2.11}$$

The function $\Delta_{\boldsymbol{q}-\boldsymbol{q}'}$ in these equations is defined by:

$$\Delta_{\boldsymbol{q}} = \Sigma_{\boldsymbol{\tau}} \delta_{\boldsymbol{q}, 2\pi\boldsymbol{\tau}}. \tag{2.12}$$

It is therefore equal to one if $\boldsymbol{q}$ is equal to any vector $2\pi\boldsymbol{\tau}$ and zero otherwise.

For a very large crystal ($\Omega \to \infty$) it becomes necessary to replace all sums over wave vectors, such as appear in equation (2.10), by integrations. We shall introduce a notation which is particularly suited to this limit; it is based on the following definitions:

$$(8\pi^3/\Omega)\, \Sigma_{\boldsymbol{q}} = \int_{\boldsymbol{q}}, \tag{2.13}$$

$$(\Omega/8\pi^3)\, \Delta_{\boldsymbol{q}} = \Delta(\boldsymbol{q}), \tag{2.14}$$

$$(\Omega/8\pi^3)^{\frac{1}{2}}\, a_{\boldsymbol{q}j} = A_{\boldsymbol{q}j}. \tag{2.15}$$

The quantity $8\pi^3/\Omega$ is the volume of $\boldsymbol{q}$-space per wave vector, the symbol $\int_{\boldsymbol{q}}$ becomes $\int \mathrm{d}\boldsymbol{q}$ in the limit $\Omega \to \infty$. The integration must be extended over the first Brillouin zone. The generalized delta-function $\Delta(\boldsymbol{q})$ defined in (2.14) has the following property

$$\int_{\boldsymbol{q}} \Delta(\boldsymbol{q}) = 1. \tag{2.16}$$

In the limit of large Ω it can be replaced as follows:

$$\Delta(\boldsymbol{q}) = \Sigma_{\boldsymbol{\tau}} \delta(\boldsymbol{q} + 2\pi\boldsymbol{\tau}). \tag{2.17}$$

The only non zero commutation rules for the operators $A_{\boldsymbol{q}j}$ and $A^*_{\boldsymbol{q}j}$, defined in equation (2.15), are

$$[A_{\boldsymbol{q}j}, A^*_{\boldsymbol{q}'j'}] = \delta_{jj'}\Delta(\boldsymbol{q} - \boldsymbol{q}'). \tag{2.18}$$

In this new notation equation (2.10) takes the following form:

$$\boldsymbol{u}_{sn} = (v_0/16\pi^3 m_n)^{\frac{1}{2}} \Sigma_j \int_{\boldsymbol{q}} \omega_{\boldsymbol{q}j}^{-\frac{1}{2}} [A_{\boldsymbol{q}j} + A^*_{-\boldsymbol{q}j}] \, (\boldsymbol{e}^{(n)}_{\boldsymbol{q}j} - i\boldsymbol{f}^{(n)}_{\boldsymbol{q}j}) \exp[i\boldsymbol{q}\cdot\boldsymbol{s}]. \tag{2.19}$$

Here $v_0 = \Omega/N_0$ is the volume of the unit cell.

The excited states (phonon states) of the harmonic Hamiltonian $|\boldsymbol{q}j, \boldsymbol{q}'j', \boldsymbol{q}''j'', \ldots\rangle$ will be defined by the following equation, which at the same time fixes the normalizing constants:

$$|\boldsymbol{q}j, \boldsymbol{q}'j', \boldsymbol{q}''j'', \ldots\rangle = A^*_{\boldsymbol{q}j} A^*_{\boldsymbol{q}'j'} A^*_{\boldsymbol{q}''j''} \ldots |0\rangle. \tag{2.20}$$

In this equation the symbol $|0\rangle$ designates the vacuum (no phonon) state.

From equations (2.18) and (2.20) it follows that the effect of an annihilation operator $A_{\boldsymbol{q}j}$ acting on a phonon state is expressed by the following equation:

$$A_{\boldsymbol{q}j} |\alpha\rangle = n_{\boldsymbol{q}j}\Delta(0) \, |\beta\rangle, \tag{2.21}$$

where state $|\alpha\rangle$ contains $n_{\boldsymbol{q}j}$ phonons $\boldsymbol{q}j$ and where state $|\beta\rangle$ has one phonon $\boldsymbol{q}j$ less than state $|\alpha\rangle$. From equation (2.14) it follows, that the quantity $\Delta(0)$ is equal to $\Omega/8\pi^3$, the density of wave vectors in $\boldsymbol{q}$-space.

If the anharmonic energy V is sufficiently small, the concept of phonons is still meaningful and V can be regarded as causing interactions between the phonons. The effect of V can in this case be investigated by means of perturbation theory. We can express V in the creation and annihilation operators $A^*_{\boldsymbol{q}j}$ and $A_{\boldsymbol{q}j}$ by substituting eq. (2.19) in eqs. (2.7) and (2.8). The total Hamiltonian for the crystal now takes the following form

$$H = \varepsilon_0 + \varepsilon_{zp} + H_0 + V. \tag{2.22}$$

Here ε_{zp} is the zero point energy of the crystal and H_0 and V are given by the following equations:

$$H_0 = \Sigma_j \int_{\boldsymbol{q}} \omega_{\boldsymbol{q}j} A^*_{\boldsymbol{q}j} A_{\boldsymbol{q}j}; \; V = \Sigma_{\nu=3}^{\infty} V^{(\nu)}, \tag{2.23}$$

with

$$V^{(\nu)} = \Sigma_{j_1 \ldots j_\nu} \int_{\boldsymbol{q}_1 \ldots \boldsymbol{q}_\nu} B^{(\nu)}_{\boldsymbol{q}_1 j_1, \ldots, \boldsymbol{q}_\nu j_\nu} [A_{\boldsymbol{q}_1 j_1} + A^*_{-\boldsymbol{q}_1 j_1}] \ldots [A_{\boldsymbol{q}_\nu j_\nu} + A^*_{-\boldsymbol{q}_\nu j_\nu}] \, \Delta(\boldsymbol{q}_1 + \ldots + \boldsymbol{q}_\nu). \tag{2.24}$$

The Δ-function in equation (2.24) arises from the summation over $\boldsymbol{s}$. The quantity $B^{(\nu)}_{\boldsymbol{q}_1 j_1 \ldots \boldsymbol{q}_\nu j_\nu}$ is essentially the Fourier transform of the coefficient $C^{(\nu)}_{s_1 n_1 \alpha_1, \ldots, s_\nu n_\nu \alpha_\nu}$; $B^{(\nu)}_{\boldsymbol{q}_1 j_1 \ldots \boldsymbol{q}_\nu j_\nu}$ is invariant under permutations of its index pairs

$\boldsymbol{q}j$; it is changed into its complex conjugate by an inversion of all its wave vectors. $B^{(\nu)}_{\boldsymbol{q}_1 j_1, \ldots, \boldsymbol{q}_\nu j_\nu}$ contains a factor $(\omega_{\boldsymbol{q}_1 j_1} \ldots \omega_{\boldsymbol{q}_\nu j_\nu})^{-\frac{1}{2}}$ which can become infinite when one of the $\omega_{\boldsymbol{q}j}$'s becomes zero, that is when $\omega_{\boldsymbol{q}j}$ corresponds to an acoustical mode with $\boldsymbol{q} = 0 \pmod{2\pi\boldsymbol{\tau}}$. However, this situation corresponds to a pure translation of the crystal as a whole and can be excluded explicitly. Barring these situations, $B^{(\nu)}_{\boldsymbol{q}_1 j_1 \ldots \boldsymbol{q}_\nu j_\nu}$ turns out to be a finite quantity, which is, at least for a large crystal, independent of the size of the crystal.

From eq. (2.24) we see that the ν'th order term $V^{(\nu)}$ is given by a linear combination of products of ν annihilation and creation operators. Each product operating on a phonon state gives either another phonon state or zero. Because of the factor $\Delta(\boldsymbol{q}_1 + \ldots + \boldsymbol{q}_\nu)$ the new phonon state must have the same total wave vector, modulo $2\pi\boldsymbol{\tau}$, as the initial one. This selection rule on the transitions induced by $V^{(\nu)}$ is often called conservation of pseudo-momentum.

3. *The scattering function for the scattering of neutrons by the crystal.* In this section the scattering function for the scattering of neutrons by the crystal, to be defined by equations (3.1) and (3.2), will be written in a form which is particularly suited for a perturbation treatment. Since we are only interested in the coherent spectrum, we shall neglect isotope and spin effects. To every nucleus in the crystal we add a constant scattering length a.

The differential cross section at a temperature T per unit of solid angle $\mathrm{d}\Omega$ and per unit of outgoing energy $\mathrm{d}\varepsilon$ of the neutron for coherent scattering in the first Born approximation is given by the following equation[10]:

$$\frac{\mathrm{d}^2\sigma_T}{\mathrm{d}\Omega\,\mathrm{d}\varepsilon} = a^2 \frac{|\boldsymbol{k}|}{|\boldsymbol{k}_0|} S_T(\boldsymbol{\kappa}\omega), \tag{3.1}$$

with the scattering function:

$$S_T(\boldsymbol{\kappa}\omega) = Z(\beta)^{-1} \sum_{\nu_0} \exp(-\beta E_{\nu_0}) \sum_\nu |\langle \psi_\nu | T_{\boldsymbol{\kappa}} | \psi_{\nu_0} \rangle|^2 \, \delta(\omega + E_{\nu_0} - E_\nu). \tag{3.2}$$

In these equations $|\psi_{\nu_0}\rangle$ and $|\psi_\nu\rangle$ are respectively initial and final excited states of the crystal. They are eigenstates of the total Hamiltonian H, given by equation (2.4), with corresponding eigenvalues E_{ν_0} and E_ν. $\boldsymbol{k}$ is the momentum of the scattered neutron ($\hbar = 1$), $\boldsymbol{k}_0$ is the momentum of the incident neutron and $\boldsymbol{\kappa} = \boldsymbol{k}_0 - \boldsymbol{k}$ and ω are respectively the momentum and the energy transfered from the neutron to the crystal. $Z(\beta)$ is the partition function for the crystal, defined by ($\beta = 1/k_B T$):

$$Z(\beta) = \mathrm{Tr}[\exp(-\beta H)]. \tag{3.3}$$

Here the symbol "Tr" designates the trace of the operator. The quantity $Z(\beta)^{-1} \exp[-\beta E_{\nu_0}]$ gives the statistical weight of the initial states at a temperature T. The operator $T_{\boldsymbol{\kappa}}$ in the matrix element of formula (3.2) is

the operator for the neutron interaction and is given by:

$$T_{\boldsymbol{\kappa}} = \Sigma_{sn} \exp(i\boldsymbol{\kappa}\cdot\boldsymbol{r}_{sn}). \tag{3.4}$$

From formula (3.2) we see, that the scattering function $S_T(\boldsymbol{\kappa}\omega)$ depends on the exact excited eigenstates of the crystal. It is in general not possible to derive simple expressions for these eigenstates when anharmonic forces are included. However, it is possible to write $S_T(\boldsymbol{\kappa}\omega)$ in a form which does not explicitly involve the exact eigenstates $|\psi_\nu\rangle$. For that purpose we use the following relation for the δ-function in (3.2):

$$2\pi\delta(x) = \int_{-\infty}^{\infty} \mathrm{e}^{-itx}\,\mathrm{d}t.$$

We then easily find for $S_T(\boldsymbol{\kappa}\,\omega)$:

$$S_T(\boldsymbol{\kappa}\omega) =$$

$$(2\pi Z(\beta))^{-1} \int_{-\infty}^{\infty} \mathrm{d}t \exp[-it\omega]\mathrm{Tr}\{\exp[-(\beta + it)\,H]\,T_{-\boldsymbol{\kappa}} \exp[itH]\,T_{\boldsymbol{\kappa}}\}. \tag{3.5}$$

It can be verified that the dummy variable t in this equation has the significance of time[10]). Using equation (2.22) we can write (3.5) as follows:

$$S_T(\boldsymbol{\kappa}\omega) = (2\pi Z_\beta)^{-1} \int_{-\infty}^{\infty} \mathrm{d}t \exp[-it\omega] \cdot$$
$$\cdot \mathrm{Tr}\{\exp[-(\beta + it)(H_0 + V)]\,T_{-\boldsymbol{\kappa}} \exp[it(H_0 + V)]\,T_{\boldsymbol{\kappa}}\} \tag{3.6}$$

with

$$Z_\beta = \exp[\beta(\varepsilon_0 + \varepsilon_{z\beta})]\,Z(\beta) = \mathrm{Tr}\{\exp[-\beta(H_0 + V)]\}. \tag{3.7}$$

We are now led to an expression for the scattering function, which is well suited for a calculation by means of perturbation theory. Since the trace is invariant under unitary transformations we can write out the trace in a representation other than that of the exact eigenstates $|\psi_\nu\rangle$. We shall use the representation in which H_0 is diagonal, that is the representation of the phonon states $|\boldsymbol{q}_1 j_1 \ldots \boldsymbol{q}_\nu j_\nu\rangle$. In this representation the trace in (3.6) takes the form:

$$\mathrm{Tr}\{\exp[-(\beta + it)(H_0 + V)]\,T_{-\boldsymbol{\kappa}} \exp[it(H_0 + V)]\,T_{\boldsymbol{\kappa}}\} =$$
$$\Sigma_{N=0}^{\infty} (N!)^{-1} \Sigma_{j_1 \ldots j_N} \int_{\boldsymbol{q}_1 \ldots \boldsymbol{q}_N} \langle \boldsymbol{q}_N j_N \ldots \boldsymbol{q}_1 j_1 | \exp[-(\beta + it)(H_0 + V)] \cdot$$
$$\cdot T_{-\boldsymbol{\kappa}} \exp[it(H_0 + V)]\,T_{\boldsymbol{\kappa}}\,|\boldsymbol{q}_1 j_1 \ldots \boldsymbol{q}_N j_N\rangle. \tag{3.8}$$

4. *Description of the diagrams.* To calculate the matrix elements in (3.8) we need perturbation expansions in powers of V for the evolution operators $U_{-t} = \exp[-it(H_0 + V)]$ and $U_t = \exp[it(H_0 + V)]$ and for the temperature dependent operator $U_\theta = \exp[i\theta(H_0 + V)]$ where $\theta = i\beta$ is purely imaginary.

These expansions are well-known; they are given by the following equations:

$$U_{-t} = \exp[-itH_0] + \sum_{n=1}^{\infty} (-i)^n \int_0^t \mathrm{d}t_n \int_0^{t_n} \mathrm{d}t_{n-1} \ldots \int_0^{t_2} \mathrm{d}t_1 \cdot \cdot \exp[-i(t - t_n) H_0] V \exp[-i(t_n - t_{n-1}) H_0] V \ldots V \exp[-it_1 H_0], \quad (4.1)$$

$$U_t = \exp[itH_0] + \sum_{n=1}^{\infty} i^n \int_0^t \mathrm{d}t_n \int_0^{t_n} \mathrm{d}t_{n-1} \ldots \int_0^{t_2} \mathrm{d}t_1 \exp[it_1 H_0] V \ldots \ldots V \exp[i(t_n - t_{n-1}) H_0] V \exp[i(t - t_n) H_0], \quad (4.2)$$

$$U_\theta = U_{it\beta} = \exp[-\beta H_0] + \sum_{n=1}^{\infty} (-1)^n \int_0^\beta \mathrm{d}\beta_n \int_0^{\beta_n} \mathrm{d}\beta_{n-1} \ldots \int_0^{\beta_2} \mathrm{d}\beta_1 \cdot \cdot \exp[-(\beta - \beta_n) H_0] V \exp[-(\beta_n - \beta_{n-1}) H_0] V \ldots V \exp[-\beta_1 H_0]. \quad (4.3)$$

We shall expand the neutron operators $T_{\boldsymbol{\kappa}}$ an $T_{-\boldsymbol{\kappa}}$ in powers of the atomic displacements:

$$T_{\boldsymbol{\kappa}} = \sum_{sn} \exp[i\boldsymbol{\kappa} \cdot \boldsymbol{r}_{sn}] = \sum_{sn} \exp[i\boldsymbol{\kappa} \cdot (\boldsymbol{s} + \boldsymbol{R}_{0n} + \boldsymbol{u}_{sn})] = \sum_{sn} \exp[i\boldsymbol{\kappa} \cdot (\boldsymbol{s} + \boldsymbol{R}_{0n})][1 + i\boldsymbol{\kappa} \cdot \boldsymbol{u}_{sn} + \ldots + \frac{i^m}{m!} (\boldsymbol{\kappa} \cdot \boldsymbol{u}_{sn})^m + \ldots]. \quad (4.4)$$

Using the expression (2.19) for $\boldsymbol{u}_{sn}$ we find for $\boldsymbol{\kappa} \cdot \boldsymbol{u}_{sn}$:

$$\boldsymbol{\kappa} \cdot \boldsymbol{u}_{sn} = (v_0 / 16\pi^3 m_n)^{\frac{1}{2}} \sum_j \int_{\boldsymbol{q}} \omega_{\boldsymbol{q}j}^{-\frac{1}{2}} [A_{\boldsymbol{q}j} + A^*_{-\boldsymbol{q}j}] \boldsymbol{\kappa} \cdot (\boldsymbol{e}_{\boldsymbol{q}j}^{(n)} - i\boldsymbol{f}_{\boldsymbol{q}j}^{(n)}) \, \mathrm{e}^{i\boldsymbol{q} \cdot \boldsymbol{s}}. \quad (4.5)$$

For $T_{-\boldsymbol{\kappa}}$ we can find a similar formula. We see from (4.4) and (4.5) that, due to the summation over $\boldsymbol{s}$, each product of annihilation and creation operators, that occurs in the expansion of $T_{\boldsymbol{\kappa}}$ contains a factor $\Delta(\boldsymbol{\kappa} - \boldsymbol{q})$, where $\boldsymbol{q}$ is the sum of the wave vectors or pseudo-momenta of the phonons created by $T_{\boldsymbol{\kappa}}$ minus the sum of the wave vectors or pseudo-momenta of the phonons annihilated by $T_{\boldsymbol{\kappa}}$. There is thus a sort of momentum conservation which involves the real momentum of the neutron. Due to this circumstance we are justified for calling the wave vector of a phonon a pseudo-momentum.

Substituting the above expansions in the right hand side of (3.8) we see that the operator in the matrix element is a linear combination of products of operators V, $\exp[i(t_i - t_{i+1})H_0]$, $\exp[-(\beta_i - \beta_{i-1}) H_0]$, $T_{\boldsymbol{\kappa}}$ and $T_{-\boldsymbol{\kappa}}$. Moreover each operator V, $T_{\boldsymbol{\kappa}}$ and $T_{-\boldsymbol{\kappa}}$ is by virtue of (2.24), (4.4) and (4.5) itself a linear combination of products of creation and annihilation operators.

To handle these complicated expressions it is very useful to introduce diagrams, a method that has already been used very successfully in different problems of many particle physics. We shall represent each phonon by a line and each V, or better a term in some $V^{(\nu)}$ by a joining point of lines (V-vertex). Each such vertex represents the operation of a term in $V^{(\nu)}$ on the state to the right of the vertex. Each line entering a vertex (coming from the right) represents a phonon which will be annihilated at that vertex; each line leaving a vertex (going to the left) represents a phonon which has been created at that vertex .The total number of lines entering or leaving a V-vertex is equal to the order ν of the $V^{(\nu)}$ which that vertex represents,

and a V-vertex of ν lines is said to describe a ν'th order process (ν is at least equal to three). In each V-vertex we have conservation of pseudo-momentum (see the end of § 2). The operators T_{κ} and $T_{-\kappa}$, which have similar structure as the operators V, we shall represent by a dot with a small circle around it and we shall call these vertices neutron vertices. A diagram corresponding to a matrix element of the n-th order in V thus has n V-vertices and in general two neutron vertices. The operators $\exp[i(t_i - t_{i\pm1})\, H_0]$ and $\exp[-(\beta_i - \beta_{i-1})\, H_0]$ act on the intermediate states between the vertices. Each diagram, just as the corresponding matrix element, has to be read from right to left starting with the state $|\boldsymbol{q}_1 j_1 \ldots \boldsymbol{q}_N j_N\rangle$ and ending with the state $\langle \boldsymbol{q}_N j_N \ldots \boldsymbol{q}_1 j_1|$. The order of the vertices in each diagram is important; it is given by the time order and the order in the β_i's in the expansions (4.1)–(4.3).

As an example we consider the following matrix element of the 5'th order in V:

$$\begin{aligned}
&\langle \boldsymbol{q}_4 j_4, \ldots, \boldsymbol{q}_1 j_1| \{-\textstyle\int_0^{\beta} \mathrm{d}\beta_1 \exp[-(\beta - \beta_1)\, H_0]\, V \exp[-\beta_1 H_0]\} \cdot \\
&\quad \cdot \{-\textstyle\int_0^t \mathrm{d}t_2 \int_0^{t_2} \mathrm{d}t_1 \exp[-i(t-t_2)H_0] V \exp[-i(t_2-t_1)\, H_0] V \exp[-it_1 H_0]\} T_{-\kappa} \cdot \\
&\quad \cdot \{\textstyle\int_0^t \mathrm{d}t_2' \int_0^{t_2'} \mathrm{d}t_1' \exp[it_1' H_0]\, V \exp[i(t_2' - t_1')\, H_0]\, V \exp[i(t - t_2')\, H_0]\} \cdot \\
&\quad \cdot T_{\kappa} |\boldsymbol{q}_1 j_1, \ldots, \boldsymbol{q}_4 j_4\rangle. \qquad (4.6)
\end{aligned}$$

For every choice of terms out of the operators V and out of T_{κ} and $T_{-\kappa}$ there is a finite number of diagrams that contributes to the above matrix element. In fig. 1 we have drawn two diagrams corresponding to different choices of terms out of V and $T_{\pm\kappa}$. For the phonon $\boldsymbol{q}_\nu j_\nu$ at the left and right of the diagram stands a number ν. The set of initial phonons is identical to the set of final phonons. A diagram which differs from the diagrams in fig. 1 by an interchange at the left and right of the role of two phonons, for instance 1 and 2, is taken as a different diagram. As will be seen from fig. 1 each diagram consists of three regions, viz. for U_t, U_{-t} and U_θ, which are separated by the dashed lines.

The diagrams described above can be imagined to be rolled onto a cylinder in such a way that each external line ν at the right of the diagram joins continuously on the back of the cylinder onto the external line for the same phonon ν at the left side of the diagram. Every line on the cylinder joining two vertices corresponds to an associated pair of a creation and an annihilation operator. Associated pairs may belong to the same vertex. A part of the diagram which is connected *on the cylinder* is called a component or connected part of the diagram. A diagram which consists of just one component is called a connected diagram. For instance, the diagram in fig. 1*a* consists of two components, one component containing the phonons 1,2 and 4 and the other containing the phonon 3; diagram *b* is connected.

The concepts of diagrams on a cylinder and connectedness on a cylinder have already been used by Bloch and De Dominicis[11]) and Van Hove[12]) for calculating partition functions.

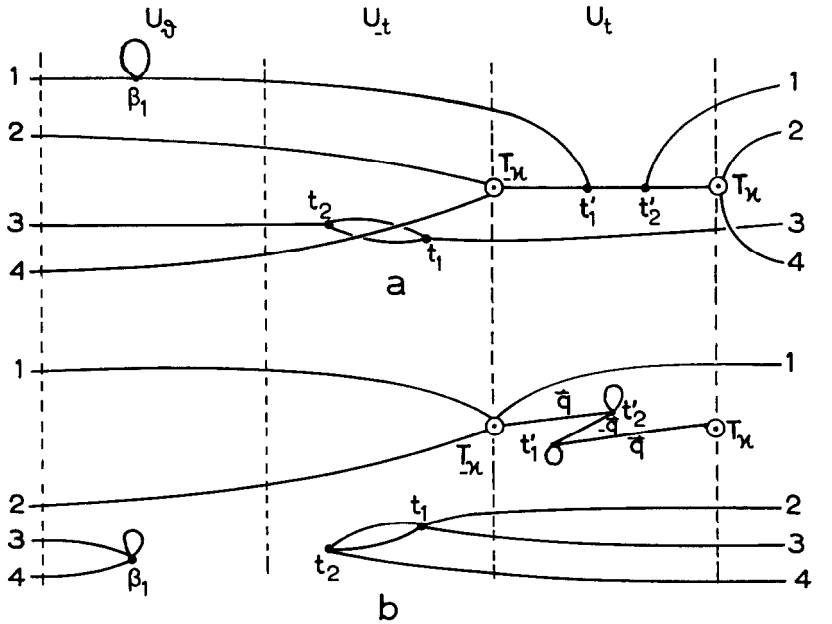

Fig. 1. Two diagrams that contribute to the matrix element (4.6).

There is an important theorem, well known from field theory and many particle perturbation theory, which states that the contribution of a diagram to a matrix element can be determined from the contributions of its components[12])[8]). In our case this theorem may be formulated as follows:

Consider a diagram containing l components. Take the sum of the contributions of this diagram and of all diagrams that arise from the original diagram by changing the relative order of the V-vertices of the different components in such a way that each V-vertex remains in the region (U_t, U_{-t} or U_θ) in which it finds itself in the original diagram. The abovementioned sum equals the product of the contributions of the l separate components times a combinatorial factor which is equal to $N!/\Pi_i(N_i!)$. Here N is the number of external lines of the total diagram and N_i is the number of external lines of the i'th component.

A diagram may contain components, which do not involve neutron vertices. Consider a diagram which contains only components with neutron vertices; such a diagram has at most two components. Consider all the other diagrams which can be constructed from the first by adding components in the above sense without neutron vertices. According to the theorem just stated the total contribution of this set of diagrams is equal

to the contribution of the original diagram times the sum of the contributions of all possible diagrams without neutron vertices; this latter sum is equal to $\mathrm{Tr}\{\exp[-\beta(H_0 + V)]\} = Z_\beta$, which may be seen from equation (3.8). This factor Z_β cancels the Z_β in the denominator of (3.6) and we thus find for the scattering function:

$$S_T(\boldsymbol{\kappa}\omega) = (2\pi)^{-1} \int_{-\infty}^{\infty} \mathrm{d}t \exp[-it\omega) \sum_\delta^{\text{neutron}} \mathrm{Tr}\{\exp[-(\beta + it)(H_0 + V)]\, T_{-\boldsymbol{\kappa}} \cdot \cdot \exp[it(H_0 + V)]\, T_{\boldsymbol{\kappa}}\}_\delta. \quad (4.7)$$

Here the symbol $\sum_\delta^{\text{neutron}}$ means that the summation is restricted to diagrams δ, which contain only components with neutron vertices.

5. *Partial scattering functions.* The diagrams that contribute to the trace in equation (4.7) can be distinguished into two types, namely (*a*) diagrams that consist of two components, each component containing one neutron vertex, and (*b*) diagrams that consist of a single component which involves both of the neutron vertices.

The diagrams of type (*a*) produce the *elastic* scattering spectrum. It is easy to see that in this case each component gives a non-zero contribution only if $\boldsymbol{\kappa} = 0 \pmod{2\pi\boldsymbol{\tau}}$. The partial scattering function $S_T^{(0)}(\boldsymbol{\kappa}\omega)$, describing the elastic spectrum, can be shown to be:

$$S_T^{(0)}(\boldsymbol{\kappa}\omega) = (8\pi^3 N_0/v_0)\, |\sum_n \exp(i\boldsymbol{\kappa}\cdot\boldsymbol{R}_{0n}) \cdot \cdot \sum_\nu Z(\beta)^{-1} \exp(-\beta E_\nu)\, \langle\psi_\nu\, |\exp(i\boldsymbol{\kappa}\cdot\boldsymbol{u}_{0n})|\, \psi_\nu\rangle|^2\, \Delta(\boldsymbol{\kappa})\, \delta(\omega).$$

From this result we conclude, that also for an anharmonic crystal the Bragg conditions are exactly valid. The sum over ν of the term in absolute value signs is the Debye-Waller factor at temperature T for the anharmonic crystal. Anharmonic forces, then, can only affect the intensity of the elastic scattering.

The *inelastic* scattering spectrum is obtained from the diagrams of type (*b*). In this paper, however, we are not interested in the complete inelastic spectrum; our aim is to study the scattering peaks, i.e. the most singular parts of the spectrum. If these most singular parts can be distinguished from the background, or in other words, if the condition $\Gamma(\boldsymbol{q})/\omega_{\boldsymbol{q}} \ll 1$, discussed in § 1, is satisfied, a part of the scattering function $S_T(\boldsymbol{\kappa}\omega)$ can be isolated which is expected to describe the desired peaks. This isolated contribution, which will be called $S_T^{(1)}(\boldsymbol{\kappa}\omega)$, can be obtained by further restricting the summation in (4.7) to diagrams belonging to a certain class. Following Van Hove[7]) we define this class as the set of all one-component diagrams, which contain at least one phonon line in the U_t- or U_{-t}-region in such a way that the diagrams disintegrate into two parts, each part containing one neutron vertex, if such a phonon line is broken. It includes the diagram in fig. 1*b*, but not that in fig. 1*a*. In the following these diagrams

will be called *one-phonon diagrams*, because in the harmonic approximation they become identical with those diagrams which exactly describe the delta-function peaks in the spectrum (see the end of this section). We must emphasize, however, that this term is somewhat misleading. As will be seen later the function $S_T^{(1)}(\boldsymbol{\kappa}\omega)$ does describe the width and location of the scattering peaks, but it describes parts of the background as well. It is by no means equivalent to a "one-phonon scattering function" in a phonon expansion. Such an expansion does not exist in the case of scattering by an anharmonic crystal (see the second footnote of § 1). Therefore it is not possible to draw conclusions about the intensity of the scattering from the partial scattering function $S_T^{(1)}(\boldsymbol{\kappa}\omega)$; this can only be done after calculating the total inelastic spectrum. It will become clear from the following sections, that the diagrams of class (*b*), which do not belong to the special class described above, only contribute to the smooth background (barring possible logarithmic singularities which we neglect here (see § 1)).

In the case of a harmonic crystal the diagrams that contribute to the trace in (4.7) become very simple. The diagrams of class (*a*), giving the elastic spectrum, consist of the two neutron vertices with phonon lines which begin and end on the same neutron vertex (loops). In addition to this the diagrams of class (*b*) contain one or more lines which connect the neutron vertices. If the number of these lines is n, the diagram in question exactly describes a n-phonon process, i.e. a process in which n phonons are involved per single scattering event. This can be seen directly by calculating the diagrams according to the rules explained in § 4. By means of this we have obtained a disjoint splitting of the set of diagrams into subsets, each subset being determined by a certain value of n ($n = 0, 1, 2, \ldots$), which immediately leads to the well-known phonon expansion derived earlier by several authors[1)3)]. The loops on the neutron vertices can be shown to yield the Debye-Waller factor for the harmonic crystal. The diagrams in which the neutron vertices are connected by a single line describe exactly the one-phonon processes. They produce a delta-function peak in the spectrum. These diagrams are the counterparts in the unperturbed system of the one-phonon diagrams defined above for the anharmonic crystal, and it follows that for a harmonic lattice $S_T^{(1)}(\boldsymbol{\kappa}\omega)$ exactly describes the scattering peaks. In the presence of anharmonic forces $S_T^{(1)}(\boldsymbol{\kappa}\omega)$ is still expected to describe these peaks, as long as the condition $\Gamma(\boldsymbol{q})/\omega_{\boldsymbol{q}} \ll 1$ is fulfilled.

6. *The structure of the one-phonon diagrams.* According to § 5 the partial scattering function $S_T^{(1)}(\boldsymbol{\kappa}\omega)$, which describes the peaks of the inelastic scattering spectrum, is obtained from (4.7) by restricting the summation to connected diagrams, of which the minimum number of phonon lines in the U_t- or U_{-t}-region, which has to be broken for making the diagram disconnected in the sense of the preceding section, is one. Let us call such lines in the one-phonon diagrams q-lines. Every one-phonon diagram will contain at least one q-line. For instance, the one-phonon diagram of fig. 1*b* has three q-lines. As a consequence of conservation of pseudo-momentum at each V-vertex, each q-line represents a phonon with wave vector $\boldsymbol{q}$ or $-\boldsymbol{q}$ (see fig. 1*b*).

Consider a one-phonon diagram with several q-lines. Let us further consider a part of the diagram which would become disconnected from the rest of the diagram if two of the, not necessarily successive, q-lines were broken. In fig. 2 we have represented schematically such a subdiagram by a shaded area; we have omitted the rest of the diagram. The points A and C, representing the vertices at which the q-lines are attached to the subdiagram, are situated in this case in the U_t-region, but this is of course not necessary.

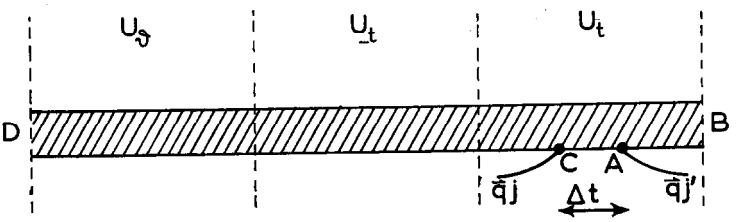

Fig. 2. A subdiagram between two q-lines.

The shaded area represents a complicated connected set of phonon lines and V-vertices in such a way that each external line at B can be continuously joined onto an external line for the same phonon at D on the back of the cylinder, according to the definition of q-line. This means that each such subdiagram itself would contribute to a trace, were it not for its connection with the rest of the diagram. As we see in fig. 2 it is only connected directly with the rest of the diagram by means of the q-lines at points A and C. There is, however, an indirect but much more complicated connection between the subdiagram and the rest of the total diagram caused by the ordered integrations in the expansions (4.1)–(4.3). As in the case of diagrams consisting of more than one component, however, we can *disentangle* different parts of the one-phonon diagrams by means of a certain permutation of V-vertices. In the case under consideration we can loosen the branches AB and CD of the subdiagram from those parts of the rest of the diagram which are situated on the right of A and on the left of C by adding to the diagram all possible diagrams which only differ from the original one in different orders of the V-vertices of the branches AB and CD with respect to those of the rest of the diagram on the right of A and on the left of C, in such a way that each V-vertex remains in its own region. The same thing we can do for part AC of the subdiagram. In both cases the vertices at A and C remain fixed. Now the sum of the contributions of this group of "permuted" diagrams is equal to the contribution of the original diagram, however, with the subdiagram disentangled from the rest of the diagram. There only remains the direct connection by means of the q-lines, the indirect connection mentioned above has been removed by taking the class of "permuted" diagrams as a whole.

The proof of the disentanglement theorem used above runs along similar

lines as the well-known proofs of theorems like the one given in § 4. In the appendix we have illustrated the theorem by means of a simple example.

The total value of all possible disentangled subdiagrams between two, not necessarily successive, q-lines in such a way that the relative positions of the two vertices at which the abovementioned q-lines enter or leave the subdiagram (points A and C in fig. 2) are fixed and are situated in the regions U_t, U_{-t} or in both, will now be given by the following expression:

$$\mathrm{Tr}\{\exp[-(\beta + i\Delta t)(H_0 + V)]\, V_{qj} \exp[i\Delta t(H_0 + V)]\, V_{qj'}\}_C . \quad (6.1)$$

Here the operators V are provided with the index pairs qj and qj' to indicate that each term from each of these operators contains either an annihilation operator or a creation operator for the phonons $\pm qj$ and $\pm qj'$ respectively. The suffix C means that only connected diagrams are involved in the calculation of the trace. Δt is the time difference between the vertices V_{qj} and $V_{qj'}$; according to (4.1) and (4.2), it may be positive or negative. Similar expressions are valid for subdiagrams which contain a neutron vertex. In this case the subdiagram involves one V_{qj}-vertex only. We shall meet them later on.

By means of this result we shall now be able to make a very useful analysis of our diagrams. Let us define a V-bubble as a subdiagram in the above sense between two successive q-lines (proper part), so the bubble itself does not contain any q-line. The general expression representing the total (time dependent) contribution of all V-bubbles with fixed relative positions of the vertices V_{qj} and $V_{qj'}$ in the regions U_t, U_{-t} or in both, can, after the disentanglement process, be written as follows (see (6.1)):

$$\mathrm{Tr}\{\exp[-(\beta + i\Delta t)(H_0 + V)]\, V_{qj} \exp[i\Delta t(H_0 + V)]\, V_{qj'}\}_{C,nq} , \quad (6.2)$$

the subscript nq meaning that the diagrams involved do not contain any q-line. In addition to V-bubbles, which only contain V-vertices, bubbles exist in which one of the V_{qj}-vertices has been replaced by a neutron vertex; let us call such bubbles neutron bubbles. Each one-phonon diagram has two neutron bubbles: the T_κ- and the $T_{-\kappa}$-bubble; a neutron bubble is attached to the rest of the diagram by only one q-line. Of course the two V_{qj}-vertices of a V-bubble and the V_{qj}-vertex and neutron vertex of a neutron bubble may coincide.

The general form of the one-phonon diagrams now simply is a chain of V-bubbles connected by q-lines, a chain beginning and ending at a neutron bubble (the neutron bubble itself is meant not to belong to the chain)*). We shall call such a chain a q-chain. A q-chain is broken by cutting one of the q-lines. The one-phonon diagrams thus have the structure as indicated in fig. 3. We have represented a bubble by a shaded area; a neutron bubble has explicitly been indicated by means of the symbol for the neutron vertex.

*) In the following the bubbles are meant to be "disentangled" from each other.

As can be seen from this figure there are V-bubbles with one ingoing and one outgoing q-line, V-bubbles with two outgoing q-lines and V-bubbles with two ingoing q-lines. The neutron bubbles may have either one ingoing q-line or one outgoing q-line. The neutron bubbles represented in fig. 3 are all of a simple type. More complicated neutron bubbles arise if for instance the V_{qj}-vertex of the T_κ-bubble is situated in the U_{-t}- or U_θ-region, and which thus extend over one or more complete regions, etc.

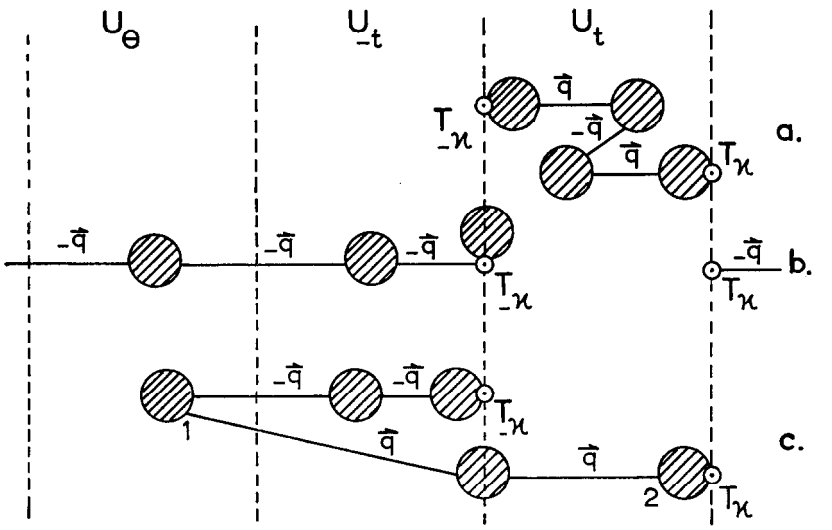

Fig. 3. General form of the one-phonon diagrams.

As will be shown in the next section the information about the shift and width of the scattering peaks is fully contained in the q-chains, which by themselves are the pure "one-phonon parts" of the diagrams. The neutron bubbles only contribute to the intensity of the scattering.

The splitting up of the one-phonon diagrams into bubbles corresponds mathematically with a splitting up of the trace on the left hand side of (3.8) (restricted to one-phonon diagrams only), into an integral over a product of exponential factors corresponding to the q-lines and of traces of the form (6.2). For this to be true it still must be proved that the factor $1/N!$ on the right hand side of (3.8) is changed into a factor $1/n!n_1!n_2!\ldots$; $n_1, n_2, \ldots$ being the numbers of external lines of each particular bubble, n being the number of external q-lines and N being the number of external lines of the total diagram. Consider a diagram without external q-lines (see fig. 3*a* and *c*). Let n_1, n_2, ..., n_ν be the numbers of external lines of the bubbles ($N = n_1 + n_2 + \ldots + n_\nu$), the diagram containing ν bubbles ($\nu - 1$ q-lines). The number of possibilities for dividing the N phonons into ν groups of n_1, n_2, ..., n_ν phonons is given by $N!/n_1!n_2!\ldots n_\nu!$. Together with the factor $1/N!$ in (3.8) this gives the required factor $1/n_1!n_2!\ldots n_\nu!$. For a diagram with external q-lines (see fig. 3*b*) a similar argument holds.

It should be noted that the bubbles introduced here have a great resemblance to the proper self-energy diagrams in field theory. Indeed, as will be seen later the bubbles describe self-energy effects which renormalize the energies of the phonons. However,

due to the dissipative character of the interaction the bubbles may involve line-broadening effects, which correspond to a finite lifetime of the phonon. Both effects are interdependent.

7. *Summation of a group of simple one-phonon diagrams.* In order to be able to perform a summation of the one-phonon diagrams, which gives an expression for the partial scattering function $S_T^{(1)}(\kappa\omega)$ in terms of the bubble functions, it is useful to make a careful classification of this set of diagrams. Let us call the q-lines by which a q-chain is attached to its "points of suspension" (the V_{qj}-vertices of the neutron bubbles) the extreme q-lines of the q-chain. Dependent on the different ways in which these extreme q-lines can be directed with respect to the "points of suspension" (the phonon represented by an extreme q-line may be either created or annihilated in the "point of suspension", or in other words each extreme q-line may run from or towards this point) we subdivide the set of q-chains between two particular neutron bubbles into the four mutually exclusive classes, which are graphically represented in fig. 4. Here the crosses are the "points of suspension" and the thick line in each diagram represents the totality of all q-chains of the

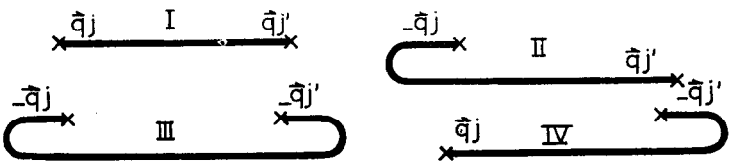

Fig. 4. Graphical representation of the four classes of q-chains.

class in question between these points. The directions of the thick lines at the "points of suspension" correspond to the directions of the extreme q-lines at these points. The q-chains of fig. 3*a*, *b* and *c*, for instance, belong to classes I, III and II respectively. The two extreme q-lines of the q-chains belonging to classes I and III may coincide; in this case the q-chain simply consists of a single line. This of course is not possible for the q-chains of classes II and IV.

If the "points of suspension" are situated in the U_t- or U_{-t}-region or in both and if Δt measures the time difference between these points, the total contribution of each of the four classes I–IV as function of this time difference, can be written as follows (see fig. 4):

$$\begin{aligned} &\text{I}: \ \mathrm{Tr}\{U_\theta U_{-\Delta t} A_{qj} U_{\Delta t} A^*_{qj'}\} c, \\ &\text{II}: \ \mathrm{Tr}\{U_\theta U_{-\Delta t} A^*_{-qj} U_{\Delta t} A^*_{qj'}\} c, \\ &\text{III}: \ \mathrm{Tr}\{U_\theta U_{-\Delta t} A^*_{-qj} U_{\Delta t} A_{-qj'}\} c, \\ &\text{IV}: \ \mathrm{Tr}\{U_\theta U_{-\Delta t} A_{qj} U_{\Delta t} A_{-qj'}\} c. \end{aligned} \tag{7.1}$$

A one-phonon diagram is said to belong to a particular class if its q-chain

belongs to that class. According to these definitions we will speak in the following of q-chains and of one-phonon diagrams of class I, II, etc. In an obvious way we can define parts of a q-chain which itself are q-chains and for these chains we can make the same classification as we did above for the total q-chains. For instance the q-chain between the points 1 and 2 of diagram c in fig. 3 belongs to class I.

The general procedure used here for summing the one-phonon diagrams is inspired by a method, introduced by Dyson[13]) in quantum electrodynamics and which has been applied by Beliaev[14]) and by Hugenholtz and Pines[15]) to their calculations on the groundstate properties of general boson systems. We have extended this method to the case of non-zero temperatures. It then turns out to be possible to perform the summation process for our diagrams without any approximation. This summation process is a complicated affair and requires a thorough analysis of the diagrams*). Before outlining it we first treat a group of relatively simple diagrams, which illustrates best some important features of the method. It consists of all diagrams which belong to class I, which have no q-lines and no V_{qj}-vertices in the U_θ-region and which contain q-lines with the same wave vector $\boldsymbol{q}$ only (so diagram a of fig. 3 does not belong to this group). Furthermore we only consider neutron bubbles of the particular type shown in fig. 5. In this figure we have schematically represented this

Fig. 5. Graphical representation of the diagrams of class I′.

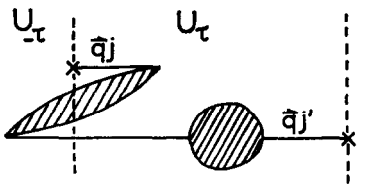

Fig. 6. A sample q-chain belonging to class I′.

group of diagrams, which we shall call in the following class I′. The wavy line represents the totality of all q-chains from class I′. An example of such a q-chain is drawn in fig. 6.

Splitting the integral over t in (4.7) into two parts, one for $t > 0$ (plus sign) and one for $t < 0$ (minus sign) we can write the total contribution $\bar{S}^{+}(\boldsymbol{\kappa}\omega)$ of the diagrams of class I′ to $S_T^{(1)}(\boldsymbol{\kappa}\omega)$ for $t > 0$ in the following form (see fig. 5):

*) The author is indebted to Prof. N. M. Hugenholtz and Dr. Th. W. Ruijgrok for valuable discussions concerning this point.

$$\bar{S}^{+}(\boldsymbol{\kappa}\omega) = (2\pi)^{-1} \sum_{j,j'} \int_{\boldsymbol{q}} \Delta(0)\, \Delta(\boldsymbol{\kappa} - \boldsymbol{q})\, i \int_0^\infty \mathrm{d}t \int_0^t \mathrm{d}t_1 \exp[-i\omega t] \cdot \cdot A_{t_1}(\boldsymbol{q}j)\, \Phi_{t-t_1}(\boldsymbol{q}jj')\, B(\boldsymbol{q}j'). \quad (7.2)$$

A similar equation holds for $t < 0$. The function $\Phi_{t-t_1}(\boldsymbol{q}jj')$ in (7.2), representing the total (time dependent) contribution of all q-chains of class I', can, according to (7.1), be written as follows:

$$\Phi_{t-t_1}(\boldsymbol{q}jj') = \mathrm{Tr}\{U_\theta U_{-(t-t_1)} A_{\boldsymbol{q}j} U_{t-t_1} A^{*}_{\boldsymbol{q}j'}\}'_C, \quad (7.3)$$

where the prime outside braces indicates the fact that in calculating this trace only diagrams of class I' are involved. The contributions of the neutron bubbles $A_{t_1}(\boldsymbol{q}j)$ and $B(\boldsymbol{q}j')$ are given by the following equations:

$$A_{t_1}(\boldsymbol{q}j) = \mathrm{Tr}\{U_\theta U_{-t_1} T_{-\boldsymbol{\kappa}} U_{t_1} V_{\boldsymbol{q}j}\}_{C,nq}, \quad (7.4)$$

$$B(\boldsymbol{q}j') = \mathrm{Tr}\{U_\theta T_{\boldsymbol{\kappa},\boldsymbol{q}j'}\}_C. \quad (7.5)$$

In (7.5) the subscript $\boldsymbol{q}j'$ indicates that $T_{\boldsymbol{\kappa}}$ must create a phonon $\boldsymbol{q}j'$. The factor $\Delta(0)\, \Delta(\boldsymbol{\kappa} - \boldsymbol{q})$ in (7.2) arises from the identity

$$[\Delta(\boldsymbol{\kappa} - \boldsymbol{q})]^2 = \Delta(0)\, \Delta(\boldsymbol{\kappa} - \boldsymbol{q}),$$

each neutron bubble contributing a factor $\Delta(\boldsymbol{\kappa} - \boldsymbol{q})$; according to (2.14) $\Delta(0)$ equals $\Omega/8\pi^3$.

Introducing in (7.2) new time variables as follows:

$$t - t_1 = \tau_2;\ t_1 = \tau_1;\ \tau_1 \geq 0,\ \tau_2 \geq 0, \quad (7.6)$$

we see that $\int_0^\infty \mathrm{d}t \int_0^t \mathrm{d}t_1$ can be replaced by $\int_0^\infty \mathrm{d}\tau_2 \int_0^\infty \mathrm{d}\tau_1$. Performing the integration over $\boldsymbol{q}$ we find for $\bar{S}^{+}(\boldsymbol{\kappa}\omega)$:

$$\bar{S}^{+}(\boldsymbol{\kappa}\omega) = (\Omega/8\pi^3) \sum_{j,j'} A^{+}(\boldsymbol{\kappa}\omega j)\, \bar{C}^{+}(\boldsymbol{\kappa}\omega jj')\, B(\boldsymbol{\kappa}j'), \quad (7.7)$$

with

$$A^{+}(\boldsymbol{\kappa}\omega j) = i \int_0^\infty \mathrm{d}\tau A_\tau(\boldsymbol{\kappa}j) \exp[-i\omega\tau], \quad (7.8)$$

and

$$\bar{C}^{+}(\boldsymbol{\kappa}\omega jj') = (2\pi)^{-1} \int_0^\infty \mathrm{d}\tau \Phi_\tau(\boldsymbol{\kappa}jj') \exp[-i\omega\tau], \quad (7.9)$$

and so we have obtained an expression for $\bar{S}^{+}(\boldsymbol{\kappa}\omega)$ which simply is the product of the contributions of the neutron bubbles and that of the q-chains. We shall now further investigate the function $\bar{C}^{+}(\boldsymbol{q}\omega jj')$ and try to express this function in terms of the contributions of the V-bubbles. Each diagram that contributes to the trace in (7.9) (see (7.3)), being a q-chain of class I', we split up into the two parts indicated in fig. 7*a*: the q-line representing the phonon $\boldsymbol{q}j$ (annihilated by $A_{\boldsymbol{q}j}$) and the rest of the diagram (the dashed line). The dot designates the vertex $V_{\boldsymbol{q}j}$ which creates the phonon $\boldsymbol{q}j$.

We can write $\bar{C}^{+}(\boldsymbol{q}\omega jj')$ as follows:

$$\bar{C}^{+}(\boldsymbol{q}\omega jj') = (2\pi)^{-1} \int_0^\infty \mathrm{d}\tau \exp[i\tau(\omega_{\boldsymbol{q}j} - \omega)]\, \delta_{jj'} + + (i/2\pi) \int_0^\infty \mathrm{d}\tau \int_0^\tau \mathrm{d}\tau_1 \exp[i\omega_{\boldsymbol{q}j}\tau_1 - i\omega\tau] \mathrm{Tr}\{U_\theta U_{-(\tau-\tau_1)} V_{\boldsymbol{q}j} U_{\tau-\tau_1} A^{*}_{\boldsymbol{q}j'}\}'_C. \quad (7.10)$$

The first term on the right hand side of this equation is the contribution of the q-chain which consists of a single line. The two factors of the integrand in the second term correspond to the splitting up of the q-chains mentioned above. Changing variables analogous to (7.6) and using the formal relation:

$$\int_0^\infty \mathrm{d}\tau \exp[i\tau(\omega_{qj} - \omega)] = i(\omega_{qj} - \omega + i0)^{-1}, \tag{7.11}$$

we find:

$$\bar{C}^+(\boldsymbol{q}\omega jj') = (i/2\pi)(\omega_{qj} - \omega + i0)^{-1}\delta_{jj'} + \\ + i(\omega_{qj} - \omega + i0)^{-1}(i/2\pi)\int_0^\infty \mathrm{d}\tau' \,\mathrm{Tr}\{U_\theta U_{-\tau'} V_{qj} U_{\tau'} A^*_{qj'}\}'_C \exp[-i\omega\tau']. \tag{7.12}$$

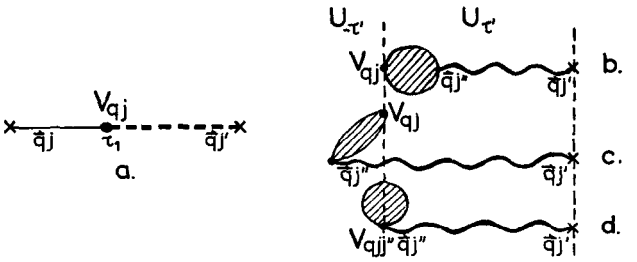

Fig. 7. The splitting up of the q-chains of class I'.

Each of the diagrams contributing to the trace in (7.12) will once more be divided into two parts: the V-bubble belonging to the V_{qj}-vertex and the rest of the diagram, which by itself is a q-chain of class I'. The three different ways in which this splitting is possible, are displayed in fig. 7*b*, *c* and *d*. In these figures the wavy lines have the same meaning as in fig. 5. Treating these diagrams in the same way as the diagrams represented in fig. 7*a*, we obtain finally the following equations for $\bar{C}^+(\boldsymbol{q}\omega jj')$ and the corresponding function $\bar{C}^-(\boldsymbol{q}\omega jj')$ for the case $t < 0$:

$$\mp 2\pi i \bar{C}^\pm(\boldsymbol{q}\omega jj') = (\omega_{qj} - \omega \pm i0)^{-1}\,\delta_{jj'} + \\ \pm 2\pi i \,\Sigma_{j''}\,(\omega_{qj} - \omega \pm i0)^{-1}\, G^\pm(\boldsymbol{q}\omega jj'')\,\bar{C}^\pm(\boldsymbol{q}\omega j''j'), \tag{7.13}$$

where either the upper sign has to be taken or the lower sign. In this equation $G^\pm(\boldsymbol{q}\omega jj'')$ is the contribution of the V-bubbles in the time independent form. It is made up of three parts corresponding to fig. 7*b*, *c* and *d* respectively (see (6.2)):

$$G^\pm(\boldsymbol{q}\omega jj'') = i\int_0^{\pm\infty} \mathrm{d}\tau \exp[-i\omega\tau]\,\mathrm{Tr}\{U_\theta U_{-\tau} V_{qj} U_\tau V_{qj''}\}_{C,nq} + \\ + i\int_0^{\mp\infty} \mathrm{d}\tau \exp[i\omega\tau]\,\mathrm{Tr}\{U_\theta U_{-\tau} V_{qj''} U_\tau V_{qj}\}_{C,nq} + \mathrm{Tr}\{U_\theta V_{qjj''}\}_C, \tag{7.14}$$

where it is to be understood that in this equation V_{qj} contains a creation operator for the phonon $\boldsymbol{q}j$, $V_{qj''}$ contains an annihilation operator for the phonon $\boldsymbol{q}j''$ and $V_{qjj''}$ contains both. It can be easily demonstrated that the function $G^\pm(\boldsymbol{q}\omega jj')$ satisfies the following relation:

$$G^\pm(\boldsymbol{q}\omega jj') = G^\mp(-\boldsymbol{q}, -\omega j'j). \tag{7.15}$$

The equations obtained for the functions $\bar{C}^{\pm}(\boldsymbol{q}\omega jj')$ are analogous to the Dyson equation in quantum electrodynamics. We have represented them graphically in fig. 8; here one should note that the diagrams in this figure now display the various quantities in the $(\boldsymbol{q}, \omega)$-representation. The shaded area represents the bubble function $G^{\pm}(\boldsymbol{q}\omega jj')$. The solution of the equations gives an expression for $\bar{C}^{\pm}(\boldsymbol{q}\omega jj')$ and thus for $\bar{S}^{\pm}(\boldsymbol{\kappa}\omega)$ in terms of the bubble functions.

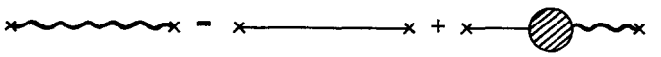

Fig. 8. Graphical representation of equations (7.13).

8. *Generalization of the summation process and discussion of the results.* Up to now we have much simplified the discussion by restricting ourselves to the special class of diagrams I'. We must now extend the results obtained so far by considering diagrams of more complicated form, such as pictured in fig. 3. First of all we consider the group of diagrams, which in addition to the diagrams of class I', consists of all diagrams which can be constructed from the diagram of fig. 5 by replacing the q-chains in this diagram by all other possible q-chains from each of the four classes I–IV. The summation of these q-chains runs along similar lines as the summation of the diagrams of class I', performed in the preceding section. Matters become very complicated in this general case, however, because of the presence of q-lines of different types (wave vectors $\boldsymbol{q}$ and $-\boldsymbol{q}$) corresponding to the possibilities of pair creation and annihilation; furthermore we must admit q-chains which have $V_{\boldsymbol{q}j}$-vertices in the U_θ-region (see fig. 3). Analogous to the notation used in § 7 we represent the total (time independent) contribution to the partial scattering function of all q-chains of class I by $C^{\pm}(\boldsymbol{q}\omega jj')$ and that of all q-chains of class II by $\tilde{C}^{\pm}(\boldsymbol{q}\omega jj')$. It is clear that $\bar{C}^{\pm}(\boldsymbol{q}\omega jj')$ is contained in $C^{\pm}(\boldsymbol{q}\omega jj')$. A careful diagram analysis, which will not be reproduced here, now leads to the following two coupled equations, analogous to (7.13) and to the Dyson equations in quantum electrodynamics, for the functions $C^{\pm}(\boldsymbol{q}\omega jj')$ and $\tilde{C}^{\pm}(\boldsymbol{q}\omega jj')$:

$$\mp 2\pi i C^{\pm}(\boldsymbol{q}\omega jj') = (\omega_{\boldsymbol{q}j} - \omega \pm i0)^{-1} f'(\boldsymbol{q}j)\delta_{jj'} + (\omega_{\boldsymbol{q}j} - \omega \pm i0)^{-1}\Theta^{\pm}(\boldsymbol{q}\omega jj') + \pm 2\pi i \sum_{j''} (\omega_{\boldsymbol{q}j} - \omega \pm i0)^{-1} G^{\pm}(\boldsymbol{q}\omega jj'')[C^{\pm}(\boldsymbol{q}\omega j''j') + \tilde{C}^{\pm}(\boldsymbol{q}\omega j''j')], \quad (8.1)$$

$$\pm 2\pi i \tilde{C}^{\pm}(\boldsymbol{q}\omega jj') = (\omega_{\boldsymbol{q}j} + \omega \mp i0)^{-1}\,\tilde{\Theta}(\boldsymbol{q}\omega jj') + \mp 2\pi i \sum_{j''} (\omega_{\boldsymbol{q}j} + \omega \mp i0)^{-1} G^{\pm}(\boldsymbol{q}\omega jj'')\,[C^{\pm}(\boldsymbol{q}\omega j''j') + \tilde{C}^{\pm}(\boldsymbol{q}\omega j''j')], \quad (8.2)$$

where again either the upper sign has to be taken or the lower sign. The quantities $f'(\boldsymbol{q}j) \equiv \{1 - \exp(-\beta\omega_{\boldsymbol{q}j})\}^{-1}$, $\Theta^{\pm}(\boldsymbol{q}\omega jj')$ and $\tilde{\Theta}^{\pm}(\boldsymbol{q}\omega jj')$ essentially represent the contributions of those parts of the diagrams which are situated in the U_θ-region. Their explicit expression is not needed for our purpose,

because they only affect the intensity of the scattering*). The quantity $G^{\pm}(\boldsymbol{q}\omega jj'')$ is defined by equation (7.14).

In fig. 9 we have graphically represented eqs. (8.1) and (8.2); the thick lines have the same meaning as in fig. 4 apart from the fact that the contributions are now written in the $(\boldsymbol{q}, \omega)$-representation; the squares designate the functions $\Theta^{\pm}(\boldsymbol{q}\omega jj')$ and $\tilde{\Theta}^{\pm}(\boldsymbol{q}\omega jj')$.

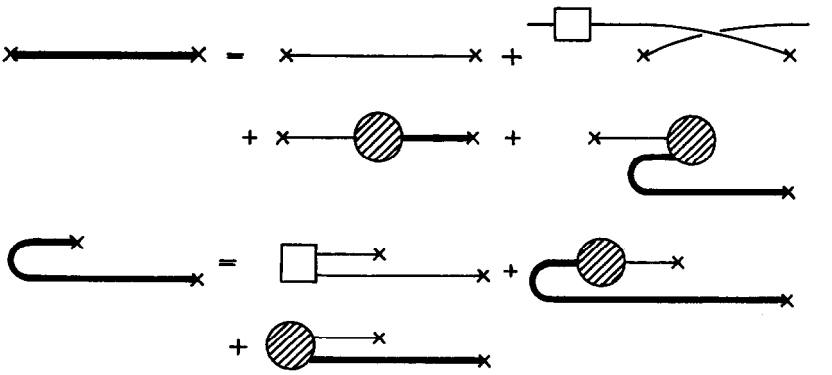

Fig. 9. The graphical representation of equations (8.1) and (8.2).

The equations obtained can be solved and one finds expressions for $C^{\pm}(\boldsymbol{q}\omega jj')$ and $\tilde{C}^{\pm}(\boldsymbol{q}\omega jj')$ in terms of the V-bubble function; the latter one describes the shift and broadening effects we are looking for, as we shall see in a moment. In exactly the same way one can find similar expressions for the functions which represent the contributions of the q-chains belonging to the classes III and IV; they only differ from $C^{\pm}$ and $\tilde{C}^{\pm}$ in the intensity factors, but give nothing new about the location and width of the scattering peaks. Having obtained expressions for the C-functions the total contribution of the group of one-phonon diagrams under study to $S_T^{(1)}(\boldsymbol{\kappa}\omega)$ can be found by substitution of these functions into equations of the form (7.7).

By doing so we have not yet obtained the correct expression for the scattering function $S_T^{(1)}(\boldsymbol{\kappa}\omega)$, because till now we have only considered diagrams with neutron bubbles of the particular type sketched in fig. 5. We must complete our considerations by including the one-phonon diagrams with all other possible types of neutron bubbles, such as have been described in § 6 for instance. A detailed investigation of these diagrams shows, however, that they only change the results obtained above by irrelevant intensity factors. Hence it is clear from the foregoing that the information concerning the effects of shifting and broadening of the peaks is fully contained in the functions $C^{\pm}(\boldsymbol{q}\omega jj')$ and $\tilde{C}^{\pm}(\boldsymbol{q}\omega jj')$ and as we are interested in these effects only, we concentrate on the functions just mentioned and leave questions of intensity out of consideration.

*) All quantities $C^{\pm}$, $\tilde{C}^{\pm}$, $G^{\pm}$, $\Theta^{\pm}$, $\tilde{\Theta}^{\pm}$, etc. depend on temperature; we shall not explicitly indicate this fact.

The equations (8.1) and (8.2) can be considered as matrix equations in which the polarization indices designate rows and columns of square matrices of order $3n_0$ (n_0 is the number of atoms per unit cell of the crystal). The calculation of the matrix elements $G^{\pm}(\boldsymbol{q}\omega jj')$, which occur in these equations, is relatively simple, at least in principle, because the contributions to these matrix elements can be easily classified as to orders of magnitude in powers of u/d and for any particular order there is only a finite number of essentially different diagrams. For instance, as we shall see in the next paragraph, the largest contributions to $G^{\pm}(\boldsymbol{q}\omega jj')$, which are of order $(u/d)^2$, only involve three essentially different diagrams [17]).

Equations (8.1) and (8.2), as they stand, are not easy to handle. To lowest order in the interaction, that is to order $(u/d)^2$, they are no longer coupled and in that case (8.1) reduces to the following equation for $C^{\pm}_{(0)}(\boldsymbol{q}\omega jj')$:

$$\mp 2\pi i \sum_{j'} [(\omega_{\boldsymbol{q}j} - \omega)\, \delta_{jj'} + G^{\pm}_{(0)}(\boldsymbol{q}\omega jj')]\, C^{\pm}_{(0)}(\boldsymbol{q}\omega j'j'') = \\ = f'(\boldsymbol{q}j)\, \delta_{jj''} + \Theta^{\pm}_{(0)}(\boldsymbol{q}\omega jj''), \qquad (8.3)$$

where the subscript (0) indicates the lowest order value ($\sim(u/d)^2$) of the quantities involved. A similar equation holds for $\tilde{C}^{\pm}_{(0)}(\boldsymbol{q}\omega jj')$. From these equations the interpretation of the functions $G^{\pm}_{(0)}(\boldsymbol{q}\omega jj')$ can be easily read off. In general the matrix $G^{\pm}_{(0)}(\boldsymbol{q}\omega jj')$ will consist of a hermitian part and an anti-hermitian part, the sign of the latter being different for G^{+} and G^{-}. If the anti-hermitian part were zero, $G^{\pm}_{(0)}(\boldsymbol{q}\omega jj')$ would have real eigenvalues. In this case the quantities $C^{\pm}_{(0)}(\boldsymbol{q}\omega jj')$ would have simple poles at various values of ω(ω is real) and the one-phonon spectrum then would consist of a number of delta-function peaks, which are shifted relative to those calculated in the harmonic approximation with the lattice parameters adjusted at the temperature considered. Because of the anti-hermitian part, however, $C^{\pm}_{(0)}(\boldsymbol{q}\omega jj')$ cannot have poles for real ω and the delta-function singularities are broadened into finite peaks. In this case the shifts of the peaks are determined by the hermitian part of $G^{\pm}_{(0)}(\boldsymbol{q}\omega jj')$, the widths by the anti-hermitian part of $G^{\pm}_{(0)}(\boldsymbol{q}\omega jj')$. In lowest order the two effects are independent of each other. Equations (8.3) describe those peaks of the scattering spectrum, whose central frequencies occur at positive values of ω and which therefore can be considered to correspond to the emission of a phonon by the neutron. Analogous equations can be written down for the absorption peaks, valid to order $(u/d)^2$.

To general order in the interaction the equations (8.1) and (8.2) must be considered together. From these equations an equation for the function $C^{\pm}(\boldsymbol{q}\omega jj') + \tilde{C}^{\pm}(\boldsymbol{q}\omega jj')$ can be derived*). We find after some algebra:

$$\mp 2\pi i \sum_{j'} [(\omega^2_{\boldsymbol{q}j} - \omega^2)\, \delta_{jj'} + 2\omega_{\boldsymbol{q}j} G^{\pm}(\boldsymbol{q}\omega jj')][C^{\pm}(\boldsymbol{q}\omega j'j'') + \tilde{C}^{\pm}(\boldsymbol{q}\omega j'j'')] = \\ (\omega_{\boldsymbol{q}j} + \omega)[f'(\boldsymbol{q}j)\, \delta_{jj''} + \Theta^{\pm}(\boldsymbol{q}\omega jj'')] - (\omega_{\boldsymbol{q}j} - \omega)\, \tilde{\Theta}^{\pm}(\boldsymbol{q}\omega jj''). \qquad (8.4)$$

*) It can be shown that the functions $C^{\pm}(\boldsymbol{\kappa}\omega jj')$ and $\tilde{C}^{\pm}(\boldsymbol{\kappa}\omega jj')$ always occur in the partial scattering function $S^{(1)}_{T}(\boldsymbol{\kappa}\omega)$ in the form $C^{\pm}(\boldsymbol{\kappa}\omega jj') + \tilde{C}^{\pm}(\boldsymbol{\kappa}\omega jj')$.

To this equation an interpretation can be given directly analogous to that of the lowest order equation (8.3). $C^{\pm}(\boldsymbol{q}\omega jj') + \tilde{C}^{\pm}(\boldsymbol{q}\omega jj')$, and therefore the scattering spectrum has maxima for those values of ω, which make the first factor within square brackets on the left hand side of (8.4) a minimum. This happens for both positive and negative values of ω. The fact that the cases $\omega > 0$ and $\omega < 0$ are both described by the same equation and are "intermixed", is a consequence of what has been said in § 1 and § 5 about the nature of the partial scattering function $S_T^{(1)}(\boldsymbol{\kappa}\omega)$. In the formalism it corresponds to the impossibility to distinguish the one-phonon diagrams into diagrams which only give contributions for $\omega > 0$ (emission) and diagrams which only give contributions for $\omega < 0$ (absorption). If $\Gamma(\boldsymbol{q})/\omega_{\boldsymbol{q}} \ll 1$, a condition which is prerequisite to the entire discussion (see § 1), the abovementioned maxima correspond to narrow well separated peaks in the scattering spectrum*), which can be interpreted as emission or absorption peaks according as their central frequencies occur at positive or negative values of ω. The various emission or absorption peaks are characterized by different values of the index j. To first order in the parameter $\Gamma(\boldsymbol{q})/\omega_{\boldsymbol{q}}$ then, it is always possible to separate the partial scattering function $S_T^{(1)}(\boldsymbol{\kappa}\omega)$ into two parts: one which describes the emission peaks, and one which describes the absorption peaks, the overlaps being of higher order in $\Gamma(\boldsymbol{q})/\omega_{\boldsymbol{q}}$.

The location and width of the peaks are determined by the quantity $G^{\pm}(\boldsymbol{q}\omega jj')$; however, in higher order in the coupling the shift and width are no longer simply the hermitian and anti-hermitian part of this quantity. More complicated expressions hold in the general case (see the end of this section). In higher order in the interaction the effects of shifting and broadening of the peaks are interdependent.

If we consider a Bravais lattice and drop the polarization indices, we get a relatively simple expression for the partial scattering function $S_T^{(1)}(\boldsymbol{\kappa}\omega)$, which clearly exhibits the features discussed above. The matrix equations (8.1) and (8.2) become in this case simple algebraic equations for the functions $C^{\pm}(\boldsymbol{q}\omega)$ and $\tilde{C}^{\pm}(\boldsymbol{q}\omega)$, which can be easily solved. In stead of the hermitian and anti-hermitian part of $G^{\pm}(\boldsymbol{q}\omega jj')$ we now have to deal with the real and imaginary part of the quantity $G^{\pm}(\boldsymbol{q}\omega)$. To first order in the parameter $\Gamma(\boldsymbol{q})/\omega_{\boldsymbol{q}}$ and putting $\Delta(\boldsymbol{\kappa}\omega) = \Delta$ and $\Gamma(\boldsymbol{\kappa}\omega) = \Gamma$, the following equation can be obtained for $S_T^{(1)}(\boldsymbol{\kappa}\omega)$, valid to general order in the interaction:

$$S_T^{(1)}(\boldsymbol{\kappa}\omega) = \frac{\Omega Q}{(\omega - \omega_{\boldsymbol{\kappa}} - \Delta)^2 + \Gamma^2} + \frac{\Omega Q'}{(\omega + \omega_{\boldsymbol{\kappa}} + \Delta)^2 + \Gamma^2}, \tag{8.5}$$

with the abbreviations

$$\Delta = \mathrm{Re}[\omega_{\boldsymbol{\kappa}}\{1 + (2G^{+}/\omega_{\boldsymbol{\kappa}})\}^{\frac{1}{2}} - \omega_{\boldsymbol{\kappa}}], \tag{8.6}$$

$$\Gamma = \mathrm{Im}[\omega_{\boldsymbol{\kappa}}\{1 + (2G^{+}/\omega_{\boldsymbol{\kappa}})\}^{\frac{1}{2}} - \omega_{\boldsymbol{\kappa}}]. \tag{8.7}$$

In $Q = Q(\boldsymbol{\kappa}\omega)$ and $Q' = Q'(\boldsymbol{\kappa}\omega)$ we have lumped together all irrelevant intensity

*) We exclude the exceptional case that the distance between the central frequencies of two emission peaks or two absorption peaks becomes of the order of the widths of the peaks.

factors. Just as Δ and Γ they depend on temperature, but they are independent of the crystal volume Ω in the limit of a large crystal.

From (8.5) we see that the spectrum exhibits in this case two peaks, one corresponding to emission and one corresponding to absorption of a phonon by the neutron, whose central frequencies occur at values $\omega = \pm(\omega_{\boldsymbol{\kappa}} + \Delta)$ and whose widths are determined by Γ. If Γ is a constant, which can be assumed to be the case if the peaks are very narrow and if Γ varies slowly with ω in Γ-neighbourhoods of $\omega = \pm(\omega_{\boldsymbol{q}} + \Delta)$, the peaks are of Lorentzian shape with widths at half maximum 2Γ.

To order $(u/d)^2$ Q' becomes zero at absolute zero, however, in higher order in the coupling (in order $(u/d)^4$ and higher) $T = 0$ does not imply $Q' = 0$. This at first sight rather strange result is a consequence of the fact already stressed at earlier stages of this work (see § 5 and the second footnote of § 1), that the partial scattering function $S_T^{(1)}(\boldsymbol{\kappa}\omega)$ in addition to the scattering peaks also describes parts of the continuous background.

If the width of each scattering peak is small compared to the value of the frequency at its centre, it is possible to establish a relation between the width of a peak and the lifetime of the phonon involved. For that purpose consider the phonon Green's function $\langle A_{\boldsymbol{q}j}(0)\, A^*_{\boldsymbol{q}j'}(t)\rangle_T$ in which the symbol $\langle\ \rangle_T$ means a statistical average at temperature T. Making use of diagram analysis we can write this function as follows:

$$\langle A_{\boldsymbol{q}j}(0) A^*_{\boldsymbol{q}j'}(t)\rangle_T = \mathrm{Tr}\{U_\theta U_{-t} A_{\boldsymbol{q}j} U_t A^*_{\boldsymbol{q}j'}\}_C\ , \tag{8.8}$$

the index C indicating as before, that in calculating the trace only connected diagrams are involved. We write $A_{\boldsymbol{q}j}$ and $A^*_{\boldsymbol{q}j'}$ for $A_{\boldsymbol{q}j}(0)$ and $A^*_{\boldsymbol{q}j'}(0)$. One immediately sees from (7.1), that the diagrams that contribute to the trace in (8.8) are the q-chains of class I. It follows that the phonon Green's function defined above, is the Fourier transform of $C^+(\boldsymbol{q}\omega jj') + C^-(\boldsymbol{q}\omega jj')$. Neglecting the difference in polarizations for convenience and then solving equations (8.1) and (8.2), we directly see that for $\Gamma(\boldsymbol{q})/\omega_{\boldsymbol{q}} \ll 1$, $C^+(\boldsymbol{q}\omega) + C^-(\boldsymbol{q}\omega)$ has the same structure as the right hand side of (8.5); it only differs from (8.5) in the numerators. To first order in the parameter $\Gamma(\boldsymbol{q})/\omega_{\boldsymbol{q}}$ we then find:

$$\langle A_{\boldsymbol{q}}(0)\, A^*_{\boldsymbol{q}}(t)\rangle_T = \{p \exp[it\Omega_{\boldsymbol{q}}] + r \exp[-it\Omega_{\boldsymbol{q}}]\} \exp[-\Gamma(\boldsymbol{q})\ |t|], \tag{8.9}$$

where we have put $\Gamma(\boldsymbol{q}\omega) \simeq \Gamma(\boldsymbol{q}\Omega_{\boldsymbol{q}}) \equiv \Gamma(\boldsymbol{q})$ with $\Omega_{\boldsymbol{q}} = \omega_{\boldsymbol{q}} + \Delta(\boldsymbol{q}\Omega_{\boldsymbol{q}})$ etc., which is justified if the peaks described by (8.5) are sufficiently narrow, and if $\Delta(\boldsymbol{q}\omega)$ and $\Gamma(\boldsymbol{q}\omega)$ are slowly varying functions of ω over the range $|\omega \pm \Omega_{\boldsymbol{q}}| \lesssim \Gamma(\boldsymbol{q})$. The factors p and r depend on wave vector and temperature. In obtaining (8.9) use has been made of the relation (7.15).

By means of this result we are able to give a significant definition of the lifetime of the phonon with wave vector $\boldsymbol{q}$ as the inverse of the quantity $\Gamma(\boldsymbol{q})$. With this definition of phonon lifetime we may say that the width of a scattering peak, if small, is equal to twice the inverse of the phonon lifetime. The same argument can be given if the polarization indices are retained. The quantity $\Omega_{\boldsymbol{q}}$, defined above, is the exact energy of the phonon $\boldsymbol{q}$ in the anharmonic crystal at temperature T.

9. *Calculation of shift and width in lowest order in the coupling.* From the preceding section it follows that to lowest order in the interaction the line shift and line width of the scattering peaks are determined by the hermitian and anti-hermitian part of the quantity $G^{\pm}(\boldsymbol{q}\omega jj')$ respectively. According to (7.14) $G^{\pm}(\boldsymbol{q}\omega jj')$ is equal to a sum of three quantities, which we shall call, in the order in which they occur in that equation, $D^{\pm}(\boldsymbol{q}\omega jj')$, $E^{\mp}(\boldsymbol{q}\omega jj')$ and

$F(\boldsymbol{q}jj')$. In lowest order these functions take the following form [17]:

$$D^{\pm}_{(0)}(\boldsymbol{q}\omega jj') = i\int_0^{\pm\infty} \mathrm{d}\tau \exp[-i\omega\tau]\, \mathrm{Tr}\{U^{(0)}_{\theta} U^{(0)}_{-\tau} V^{(3)}_{\boldsymbol{q}j} U^{(0)}_{\tau} V^{(3)}_{\boldsymbol{q}j'}\}_{C,n\boldsymbol{q}}\,, \quad (9.1)$$

$$E^{\mp}_{(0)}(\boldsymbol{q}\omega jj') = i\int_0^{\mp\infty} \mathrm{d}\tau \exp[i\omega\tau]\, \mathrm{Tr}\{U^{(0)}_{\theta} U^{(0)}_{-\tau} V^{(3)}_{\boldsymbol{q}j'} U^{(0)}_{\tau} V^{(3)}_{\boldsymbol{q}j}\}_{C,n\boldsymbol{q}}\,, \quad (9.2)$$

$$F_{(0)}(\boldsymbol{q}jj') = \mathrm{Tr}\{U^{(0)}_{\theta} V^{(4)}_{\boldsymbol{q}jj'}\}_C\,, \quad (9.3)$$

where

$$U^{(0)}_{\pm\tau} = \exp[\pm i\tau H_0],\ U^{(0)}_{\theta} = \exp[i\theta H_0] = \exp[-\beta H_0].$$

One of the diagrams that contributes to the trace in (9.1) is diagram *a* of fig. 10, which describes processes involving three phonons. The vertex on the right hand side of the diagram contains the annihilation operator for the phonon $\boldsymbol{q}j'$, the vertex on the left hand side contains the creation operator for the phonon $\boldsymbol{q}j$. We have indicated this with an incoming and outgoing arrow. In addition to diagram *a* there is a class of related diagrams, which contribute to the trace in (9.1) and which only differ from diagram *a* in the internal phonons $\boldsymbol{q}_1j_1$ and $\boldsymbol{q}_2j_2$ encircling the cylinder an arbitrary number of times while the roles of the annihilation and creation operators for these phonons may be changed in one vertex with respect to the other.

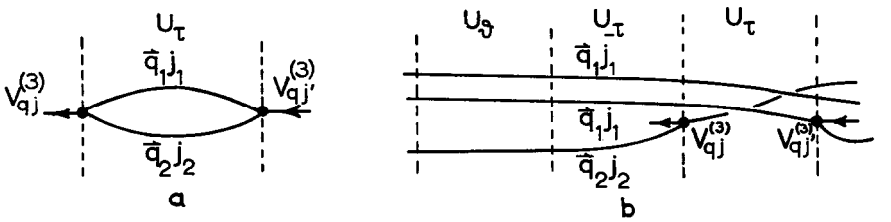

Fig. 10. Diagrams, contributing to the trace in equation (9.1).

An example of a diagram out of this class is diagram *b* in fig. 10. We see that in this diagram contrary to diagram *a* phonon $\boldsymbol{q}_2j_2$ has been created at the left hand vertex and annihilated at the right hand vertex. As has been proved for instance by Van Hove [12] for a similar case we can fully account for this whole class of diagrams by just calculating diagram *a* but replacing each factor $\exp[i\tau\omega_{\boldsymbol{q}j_i}]$ that occurs in the calculation of this diagram by $D_{\boldsymbol{q}j_i}(\tau)$, the phonon propagator, which is given by:

$$D_{\boldsymbol{q}j_i}(\tau) = \{\exp[i\tau\omega_{\boldsymbol{q}j_i}] + \exp[-(\beta + i\tau)\,\omega_{\boldsymbol{q}j_i}]\}\{1 - \exp[-\beta\omega_{\boldsymbol{q}j_i}]\}^{-1}. \quad (9.4)$$

This new propagation function now contains explicitly a correction for the presence of thermal phonons, the latter obeying Bose-Einstein statistics. The total contribution to the trace in (9.1) from all of the processes characterized by the diagrams in fig. 10, is given by the following expression:

$$18 f_{\boldsymbol{q}_1,\boldsymbol{q}_2} \Sigma_{j_1,j_2} [\Delta(\boldsymbol{q} - \boldsymbol{q}_1 - \boldsymbol{q}_2)]^2 \cdot$$
$$\cdot\, B^{(3)}_{\boldsymbol{q}j',-\boldsymbol{q}_1j_1,-\boldsymbol{q}_2j_2} B^{(3)}_{-\boldsymbol{q}j,\boldsymbol{q}_1j_1,\boldsymbol{q}_2j_2} D_{\boldsymbol{q}_1j_1}(\tau) D_{\boldsymbol{q}_2j_2}(\tau) \Delta(0)^{-1}. \quad (9.5)$$

Use has been made of equations (2.24) and (9.4). The factor 18 is a combinatorial factor, which gives the number of inequivalent ways in which the creation and annihilation operators can be permuted in each vertex with respect to each other. According to equation (2.24) two terms $V^{(3)}$ together involve six integrations over wave vectors, only two of which are actually used in expression (9.5). The four unused integrations give according to (2.13) a factor $\Delta(0)^{-4}$ ($\Delta(0) = \Omega/8\pi^3$). Furthermore we have a factor $\Delta(0)^3$ coming from the annihilation operators according to (2.21). This explains the factor $\Delta(0)^{-1}$ in (9.5). Using the identity:

$$[\Delta(\boldsymbol{q} - \boldsymbol{q}_1 - \boldsymbol{q}_2)]^2 = \Delta(0)\,\Delta(\boldsymbol{q} - \boldsymbol{q}_1 - \boldsymbol{q}_2), \tag{9.6}$$

we see that the factors $\Delta(0)$ in (9.5) cancel, giving a result independent of the volume Ω of the crystal in the limit $\Omega \to \infty$. This result also holds for the traces in (9.2) and (9.3); it remains true to all orders in the coupling. As a consequence the quantity $G^{\pm}(\boldsymbol{q}\omega jj')$ is independent of the volume in the limit $\Omega \to \infty$ in accordance with the fact that the energy shifts and the widths described by $G^{\pm}(\boldsymbol{q}\omega jj')$ are intensive quantities.

Combining (9.1), (9.4), (9.5) and (9.6) and making use of the formal relation

$$\int_0^{\mp\infty} \mathrm{d}\tau \exp[i\tau\omega] = i(1/\omega)_P \pm \pi\delta(\omega), \tag{9.7}$$

where P means the Cauchy principal value, we find:

$$\begin{aligned}
D^{\pm}_{(0)}(\boldsymbol{q}\omega jj') = 18 \int_{\boldsymbol{q}_1,\boldsymbol{q}_2} \sum_{j_1,j_2} & B^{(3)}_{\boldsymbol{q}j',-\boldsymbol{q}_1j_1,-\boldsymbol{q}_2j_2} B^{(3)}_{-\boldsymbol{q}j,\boldsymbol{q}_1j_1,\boldsymbol{q}_2j_2} \cdot \\
& \cdot \Delta(\boldsymbol{q} - \boldsymbol{q}_1 - \boldsymbol{q}_2)[\{1 - \exp[-\beta\omega_{\boldsymbol{q}_1j_1}]\}\{1 - \exp[-\beta\omega_{\boldsymbol{q}_2j_2}]\}]^{-1} \cdot \\
& \cdot \{[(\omega - \omega_{\boldsymbol{q}_1j_1} - \omega_{\boldsymbol{q}_2j_2})^{-1} + \exp[-\beta\omega_{\boldsymbol{q}_1j_1}](\omega + \omega_{\boldsymbol{q}_1j_1} - \omega_{\boldsymbol{q}_2j_2})^{-1} + \\
& \quad + \exp[-\beta\omega_{\boldsymbol{q}_2j_2}](\omega - \omega_{\boldsymbol{q}_1j_1} + \omega_{\boldsymbol{q}_2j_2})^{-1} + \\
& \quad + \exp[-\beta(\omega_{\boldsymbol{q}_1j_1} + \omega_{\boldsymbol{q}_2j_2})](\omega + \omega_{\boldsymbol{q}_1j_1} + \omega_{\boldsymbol{q}_2j_2})^{-1}]_P + \\
\pm \pi i[& \delta(\omega - \omega_{\boldsymbol{q}_1j_1} - \omega_{\boldsymbol{q}_2j_2}) + \exp[-\beta\omega_{\boldsymbol{q}_1j_1}]\,\delta(\omega + \omega_{\boldsymbol{q}_1j_1} - \omega_{\boldsymbol{q}_2j_2}) + \\
& + \exp[-\beta\omega_{\boldsymbol{q}_2j_2}]\,\delta(\omega - \omega_{\boldsymbol{q}_1j_1} + \omega_{\boldsymbol{q}_2j_2}) + \\
& + \exp[-\beta(\omega_{\boldsymbol{q}_1j_1} + \omega_{\boldsymbol{q}_2j_2})]\delta(\omega + \omega_{\boldsymbol{q}_1j_1} + \omega_{\boldsymbol{q}_2j_2})]\}.
\end{aligned} \tag{9.8}$$

We see immediately from the last equation, taking into account the properties of the coefficients $B^{(3)}$ mentioned in § 2, that we have obtained a separation of $D^{\pm}_{(0)}(\boldsymbol{q}\omega jj')$ in a hermitian and an anti-hermitian part.

The only basic diagram that contributes to the trace in (9.2) is given in fig. 11*a*. The vertex on the right hand side now contains the creation operator for the phonon $\boldsymbol{q}j$, the one on the left hand side contains the annihilation operator for the phonon $\boldsymbol{q}j'$. To include related diagrams analogous to the one in fig. 10*b* we must also in this case use the phonon propagator function (9.4) for the internal lines corresponding to the phonons $\boldsymbol{q}_1j_1$ and $\boldsymbol{q}_2j_2$.

We then find for $E^{\mp}_{(0)}(\boldsymbol{q}\omega jj')$:

$$E^{\mp}_{(0)}(\boldsymbol{q}\omega jj') = 18 \int_{\boldsymbol{q}_1,\boldsymbol{q}_2} \sum_{j_1,j_2} B^{(3)}_{-\boldsymbol{q}j,-\boldsymbol{q}_1j_1,-\boldsymbol{q}_2j_2} B^{(3)}_{\boldsymbol{q}j',\boldsymbol{q}_1j_1,\boldsymbol{q}_2j_2} \cdot$$
$$\cdot \Delta(\boldsymbol{q}_1 + \boldsymbol{q}_2 + \boldsymbol{q})[\{1 - \exp[-\beta\omega_{\boldsymbol{q}_1j_1}]\}\{1 - \exp[-\beta\omega_{\boldsymbol{q}_2j_2}]\}]^{-1} \cdot$$
$$\cdot \{[-(\omega + \omega_{\boldsymbol{q}_1j_1} + \omega_{\boldsymbol{q}_2j_2})^{-1} - \exp[-\beta\omega_{\boldsymbol{q}_1j_1}](\omega - \omega_{\boldsymbol{q}_1j_1} + \omega_{\boldsymbol{q}_2j_2})^{-1} +$$
$$- \exp[-\beta\omega_{\boldsymbol{q}_2j_2}](\omega + \omega_{\boldsymbol{q}_1j_1} - \omega_{\boldsymbol{q}_2j_2})^{-1} +$$
$$- \exp[-\beta(\omega_{\boldsymbol{q}_1j_1} + \omega_{\boldsymbol{q}_2j_2})](\omega - \omega_{\boldsymbol{q}_1j_1} - \omega_{\boldsymbol{q}_2j_2})^{-1}]_P +$$
$$\mp\pi i[\delta(\omega + \omega_{\boldsymbol{q}_1j_1} + \omega_{\boldsymbol{q}_2j_2}) + \exp[-\beta\omega_{\boldsymbol{q}_1j_1}]\,\delta(\omega - \omega_{\boldsymbol{q}_1j_1} + \omega_{\boldsymbol{q}_2j_2}) +$$
$$+ \exp[-\beta\omega_{\boldsymbol{q}_2j_2}]\,\delta(\omega + \omega_{\boldsymbol{q}_1j_1} - \omega_{\boldsymbol{q}_2j_2}) +$$
$$+ \exp[-\beta(\omega_{\boldsymbol{q}_1j_1} + \omega_{\boldsymbol{q}_2j_2})]\,\delta(\omega - \omega_{\boldsymbol{q}_1j_1} - \omega_{\boldsymbol{q}_2j_2})]\}, \quad (9.9)$$

where we have again obtained a separation in hermitian and anti-hermitian parts. Diagram b in fig. 11, describing an "instantaneous" phonon,

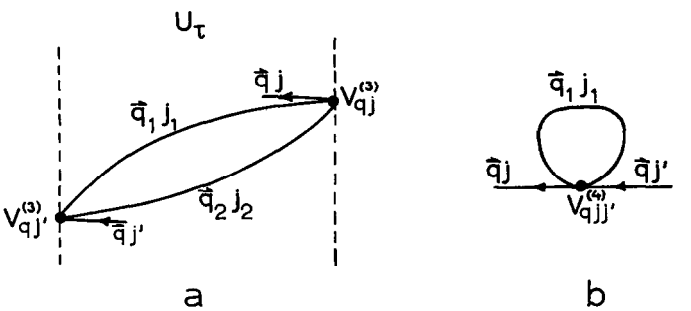

Fig. 11. Diagrams contributing to the traces in (9.2) and (9.3).

contributes to the trace in (9.3). We find for $F_{(0)}(\boldsymbol{q}jj')$, calculated from this diagram and the class of related diagrams:

$$F_{(0)}(\boldsymbol{q}jj') =$$
$$= 12 \int_{\boldsymbol{q}_1} \sum_{j_1} B^{(4)}_{\boldsymbol{q}j,-\boldsymbol{q}j',\boldsymbol{q}_1j_1,-\boldsymbol{q}_1j_1}\{1 + \exp[-\beta\omega_{\boldsymbol{q}_1j_1}]\}\{1 - \exp[-\beta\omega_{\boldsymbol{q}_1j_1}]\}^{-1} \quad (9.10)$$

From the properties of $B^{(4)}_{\boldsymbol{q}j,-\boldsymbol{q}j',\boldsymbol{q}_1j_1,-\boldsymbol{q}_1j_1}$ it follows that $F_{(0)}(\boldsymbol{q}jj')$ is hermitian. So in lowest order $F(\boldsymbol{q}jj')$ only contributes to the line shift; the only contributions to the line width come from (9.8) and (9.9), that is from expressions which only involve the cubic terms $B^{(3)}_{\cdots}$. From the right hand sides of (9.8), (9.9) and (9.10) we obtain formulae for the line shift $\Delta_{(0)}(\boldsymbol{q}\omega jj')$ and the line width $2\Gamma_{(0)}(\boldsymbol{q}\omega jj')$ which are valid to order $(u/d)^2$ and which express these quantities in the parameters of the lattice. After some manipulations and using the properties of the coefficients $B^{(3)}_{\cdots}$, we get:

$$\Gamma_{(0)}(\boldsymbol{q}\omega jj') = 18\pi f_{\boldsymbol{q}_1,\boldsymbol{q}_2} \sum_{j_1,j_2} B^{(3)}_{\boldsymbol{q}j',-\boldsymbol{q}_1j_1,-\boldsymbol{q}_2j_2} B^{(3)}_{-\boldsymbol{q}j,\boldsymbol{q}_1j_1,\boldsymbol{q}_2j_2} \Delta(\boldsymbol{q}_1 + \boldsymbol{q}_2 - \boldsymbol{q}) \cdot$$
$$\cdot \{(1 + f_{\boldsymbol{q}_1j_1} + f_{\boldsymbol{q}_2j_2})[\delta(\omega - \omega_{\boldsymbol{q}_1j_1} - \omega_{\boldsymbol{q}_2j_2}) - \delta(\omega + \omega_{\boldsymbol{q}_1j_1} + \omega_{\boldsymbol{q}_2j_2})] +$$
$$+ 2(f_{\boldsymbol{q}_1j_1} - f_{\boldsymbol{q}_2j_2})\,\delta(\omega + \omega_{\boldsymbol{q}_1j_1} - \omega_{\boldsymbol{q}_2j_2})\}, \quad (9.11)$$

$$\Delta_{(0)}(\boldsymbol{q}\omega jj') = 18 f_{\boldsymbol{q}_1,\boldsymbol{q}_2} \sum_{j_1,j_2} B^{(3)}_{\boldsymbol{q}j',-\boldsymbol{q}_1j_1,-\boldsymbol{q}_2j_2} B^{(3)}_{-\boldsymbol{q}j,\boldsymbol{q}_1j_1,\boldsymbol{q}_2j_2} \Delta(\boldsymbol{q}_1 + \boldsymbol{q}_2 - \boldsymbol{q}) \cdot$$
$$\cdot \{(1 + f_{\boldsymbol{q}_1j_1} + f_{\boldsymbol{q}_2j_2})[(\omega - \omega_{\boldsymbol{q}_1j_1} - \omega_{\boldsymbol{q}_2j_2})^{-1} - (\omega + \omega_{\boldsymbol{q}_1j_1} + \omega_{\boldsymbol{q}_2j_2})^{-1}] +$$
$$+ 2(f_{\boldsymbol{q}_1j_1} - f_{\boldsymbol{q}_2j_2})(\omega + \omega_{\boldsymbol{q}_1j_1} - \omega_{\boldsymbol{q}_2j_2})^{-1}\}_P + F_{(0)}(\boldsymbol{q}jj'), \quad (9.12)$$

with

$$f_{\boldsymbol{q}j} = [\exp(\beta\omega_{\boldsymbol{q}j}) - 1]^{-1}.$$

The derived formulae exhibit an explicit dependence on temperature through the factors $f_{\boldsymbol{q}_1j_1}$ and $f_{\boldsymbol{q}_2j_2}$. As will be discussed in the next section, however, a further temperature dependence is implied by the coefficients $B^{(3)}$ and $B^{(4)}$ and the frequencies $\omega_{\boldsymbol{q}j}$ due to the effect of thermal expansion. Neglecting this latter fact it follows from (9.11) and (9.12) that for high temperatures ($T \gg T_D$) the width and shift of each scattering peak are proportional to T, in agreement with the experimental results mentioned in the introduction. For $T \to 0$ (9.11) and (9.12) become identical with the results of Van Hove[7]).

As has been stressed before (see § 1) it makes sense to calculate the shift and width to higher order in u/d by considering higher order diagrams, as long as the condition $\Gamma(\boldsymbol{q})/\omega_{\boldsymbol{q}} \ll 1$ is satisfied. We shall not do this here explicitly, because the number of diagrams to calculate increases considerably with the order. It can be seen that all the contributions to $G^{\pm}(\boldsymbol{q}\omega jj')$ are of even order, so the first higher order term of $G^{\pm}(\boldsymbol{q}\omega jj')$ is of order $(u/d)^4$. This remains true for the shift and width as can be deduced from equations (8.6) and (8.7) for instance.

10. *Closing remarks.* In this section we shall make some remarks concerning possible quantitative calculations of the effects, which are studied in this paper in an entirely formal way only. Although it does seem to be feasible, a quantitative calculation of these effects at different temperatures is expected to be a hard task for several reasons.

In the first place there is the difficulty of thermal expansion. Let us consider a Bravais lattice. Because of the anharmonic forces the equilibrium positions of the atoms in the crystal are by no means equal to those obtained by minimizing the total potential energy of the system of particles. This remains true even at absolute zero as a result of the zero-point vibrations. At every temperature T the actual equilibrium positions must be calculated by minimizing the free energy of the anharmonic crystal at temperature T with respect to the primitive translation vectors. The free energy can be calculated by the same methods as used in this paper; this has been done

by Van Hove in a formal way[7] [12]). For a more general lattice with more than one atom per unit cell the situation is even more complicated. Having calculated the actual equilibrium positions of the atoms at temperature T we must expand the potential energy in powers of the displacements of the atoms from these equilibrium positions. The expansion coefficients $C^{(\nu)}_{n_1 s_1 \alpha_1 \ldots n_\nu s_\nu \alpha_\nu}$, including $\nu = 2$ (see § 2), must be evaluated for the actual equilibrium lattice at temperature T. With these values of the coefficients the harmonic problem for that temperature must be solved. Hence at different temperatures we get different values of the coefficients $B^{(\nu)}_{q_1 j_1 \ldots q_\nu j_\nu}$ and different sets of harmonic frequencies ω_{qj}. These latter frequencies, which thus include the effects of thermal expansion, correspond to the undisturbed frequencies of our perturbation problem as formulated in § 2. The frequency variation with temperature of the scattering peaks, as measured by experiment, comprises both the effects of thermal expansion and the self-energy effects, calculated in the preceding sections.

There is another difficulty of more practical nature concerning our knowledge of the coefficients $B^{(\nu)}_{q_1 j_1 \ldots q_\nu j_\nu}$. In principle we can determine these coefficients by choosing some special interatomic force function. However, there is usually no reliable information about these force functions, except for ionic and molecular crystals. The latter type of crystal, of which the molecules cohere through van der Waals forces, is most simply represented by the rare gas solids and it is here that quantitative calculations are perhaps most feasible. Because of the weakness of the Van der Waals forces with respect to other types of binding forces, anharmonic effects are expected to be considerable even at low temperatures. Unfortunately, the simplicity of the structure is counterbalanced by the difficulty of obtaining good single crystals for experiment.

For many crystals some indirect information about the quantities $B^{(\nu)}_{q_1 j_1 \ldots q_\nu j_\nu}$ can be obtained from other data, for instance thermal expansion, thermal conductivity and the like.

In general we may say, that for performing detailed calculations of the effects discussed in this paper, which can be checked by experiments, we must choose a type of crystal, which satisfies two requirements, one of theoretical nature and one of experimental nature: *a*) from the theoretical point of view the crystal structure must be as simple as possible with as much information as possible about the atomic force constants, *b*) the crystal must be accessible to accurate measurements of the abovementioned effects, especially in the lower temperature region, i.e. it must be possible to obtain good single crystals and the cross-sections for incoherent scattering, magnetic scattering by the atomic electrons and absorption of the neutrons must be small with respect to the coherent scattering cross-section.

Then we must do the calculation according to the program outlined above. We have the intention to start such a calculation.

Acknowledgements. The author is greatly indebted to Professor L. Van Hove for his kind interest in this work, for a number of illuminating discussions and for reading the essential parts of the manuscript. The author also wishes to thank Professor B. R. A. Nijboer for his stimulating advice and criticism throughout this work.

This work is part of the research program of the "Stichting voor Fundamenteel Onderzoek der Materie", which is financially supported by the Netherlands Organization for pure Scientific Research (Z.W.O.).

Appendix

In this appendix we shall illustrate the disentanglement process, treated in § 6, by a simple example which will indicate its general validity. Consider the diagram drawn in fig. 12.; it is a one-phonon diagram containing one q-line (line b).

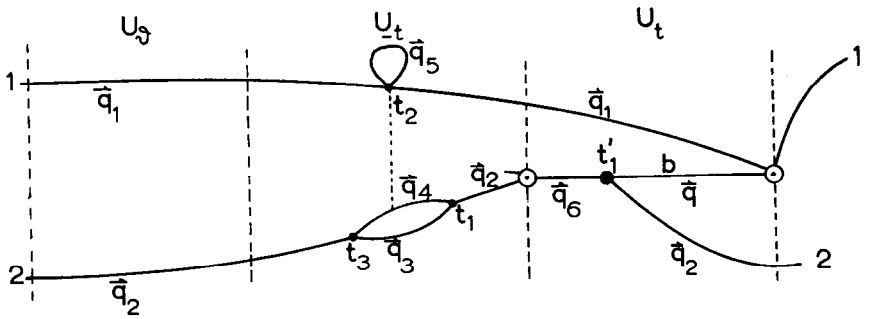

Fig. 12. One-phonon diagram with one q-line.

Cutting this q-line the diagram disintegrates into two parts, one part containing the phonon 1 (we set 1 for $\boldsymbol{q}_1$, etc.) together with the neutron vertex T_κ and the loop at t_2, and the other part containing the phonon 2 together with the neutron vertex $T_{-\kappa}$ and the V-vertices at t_1', t_1 and t_3. In addition to a direct connection between these two parts by means of the q-line (line b) there is an indirect connection caused by the ordered time integrations, i.e. by the ordering of the V-vertices of one part with respect to those of the other part. In the above diagram the only indirect connection of the two abovementioned parts is caused by the V-vertices in the U_{-t}-region; one should always have $t_1 \leqq t_2 \leqq t_3$. However, we can get rid of this indirect connection by adding to the diagram in fig. 12 the diagrams represented in fig. 13. These two diagrams only differ from the diagram in fig. 12 in different orders of the vertex at t_2 with respect to the vertices at t_1 and t_3.

The total contribution of the three diagrams of fig. 12 and 13 to the trace

in (4.7) can now be written as follows (we shall neglect polarizations for convenience):

$$\int_{q_i} K(\boldsymbol{q}_i) \exp[-\beta(\omega_1+\omega_2)][\int_0^t \mathrm{d}t_3 \int_0^{t_3} \mathrm{d}t_2 \int_0^{t_2} \mathrm{d}t_1 + \\ + \int_0^t \mathrm{d}t_2 \int_0^{t_2} \mathrm{d}t_3 \int_0^{t_3} \mathrm{d}t_1 + \int_0^t \mathrm{d}t_3 \int_0^{t_3} \mathrm{d}t_1 \int_0^{t_1} \mathrm{d}t_2] \cdot \\ \cdot \exp[-it\omega_1 - i(t-t_3)\,\omega_2 - i(t_3-t_1)(\omega_3+\omega_4) - it_1\omega_2] \cdot \\ \cdot \int_0^t \mathrm{d}t_1' \exp[it_1'\omega_6 + i(t-t_1')(\omega_2+\omega_q) + it\omega_1]. \qquad \text{(A.1)}$$

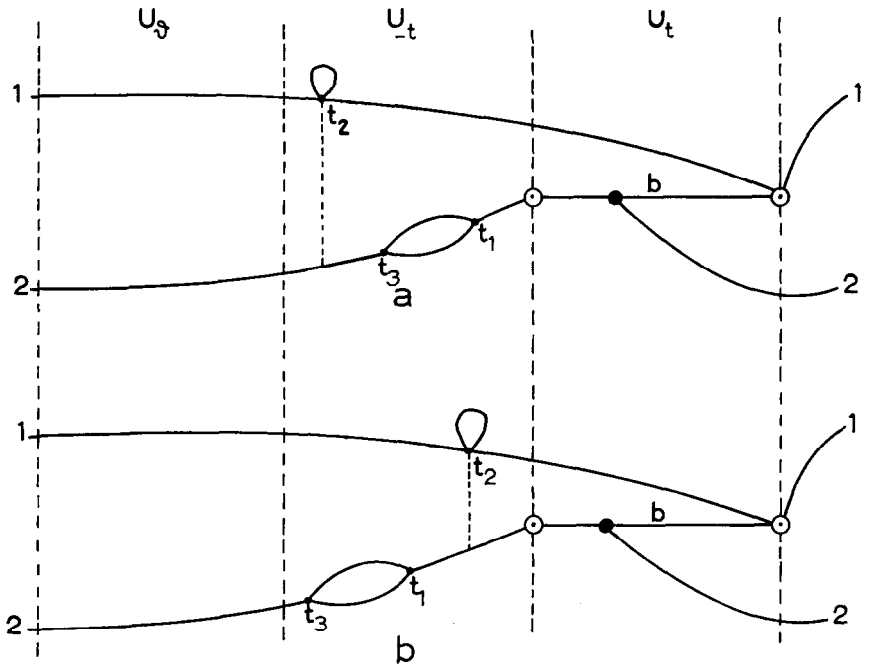

Fig. 13. Diagrams with different orders of the V-vertices in the U_{-t}-region.

In $K(\boldsymbol{q}_i)$ we have lumped together all irrelevant factors which are common to the three diagrams. The symbol $\int_{q_i}$ means that we have to sum over all wave vectors. It can easily be seen that the sum of the three integrals within square brackets can be replaced by $\int_0^t \mathrm{d}t_2 \int_0^t \mathrm{d}t_3 \int_0^{t_3} \mathrm{d}t_1$ and (A.1) becomes:

$$\int_{q_i} K(\boldsymbol{q}_i) \exp[-\beta\omega_2] \int_0^t \mathrm{d}t_3 \int_0^{t_3} \mathrm{d}t_1 \cdot \\ \cdot \exp[-i(t-t_3)\,\omega_2 - i(t_3-t_1)(\omega_3+\omega_4) - it_1\omega_2] \cdot \\ \int_0^t \mathrm{d}t_1' \exp[it_1'\omega_6 + i(t-t_1')(\omega_2+\omega_q)] \exp[-\beta\omega_1] \int_0^t \mathrm{d}t_2.$$

From this formula we see that the integration over t_2 is now independent of that over t_1 and t_3. Furthermore it can be easily seen, that the factor $K(\boldsymbol{q}_i)$ factorises into two factors, which correspond to the abovementioned

two parts of the diagram. For our simple example we have now completed the disentanglement process; only the direct connection between the two parts by means of the q-line remains (integration over t_1').

Received 19-9-61

REFERENCES

1) For a survey see:
Kothari, L. S. and Singwi, K. S., in *Solid State Physics*, edited by F. Seitz and D. Turnbull (Academic Press, New York, 1959), vol. **8**, p. 110.
2) Placzek, G. and Van Hove, L., Phys. Rev. **93** (1954) 1207.
3) Sjölander, A., Ark. f. Fys. **13** (1958) 215; **14** (1958) 315.
4) Brockhouse, B. N., Arase, T., Caglioti, G., Sakamoto, M., Sinclair, R. N. and Woods, A. D. B., Report presented at the symposium on Inelastic scattering of neutrons by solids and liquids, Vienna, October 1960.
See also: Egelstaff, P. A. and McCallum, S., Nature **181** (1958) 643.
5) Larsson, K. E., Dahlborg, U., Holmryd, S., Ark. f. Fys. **17** (1960) 369.
6) Baym, G., Phys. Rev. **121** (1961) 741.
7) Van Hove, L., *Interactions of Elastic Waves in Solids*, Solid State and Molecular Theory Group, Technical Report no. 11, Massachusetts Institute of Technology, Cambridge, Massachusetts, March 1959 (unpublished). See also: Van Hove, L., Hugenholtz, N. M. and Howland, P., *Quantum Theory of Many Particle Systems* (lecture notes and selected reprints), W. A. Benjamin, New York (1961).
8) Hugenholtz, N. M., Physica **23** (1957) 481.
9) Nosanow, L. H., Physica **26** (1960) 1124.
10) Van Hove, L., Phys. Rev. **95** (1954) 249.
11) Bloch, C. and De Dominicis, C., Nuclear Physics **10** (1959) 181.
12) Van Hove, L., Mimeographed lecture notes, University of Washington, Seattle, Wash. (1958).
13) Dyson, F. J., Phys. Rev. **75** (1949) 1736.
14) Beliaev, S. T., Soviet Phys. JETP **7** (1958) 289.
15) Hugenholtz, N. M. and Pines, D., Phys. Rev. **116** (1959) 489.
16) Kashcheev, V. N. and Krivoglaz, M. A., Soviet Phys. Solid State **3** (1961) 1107.
17) In addition to the three diagrams calculated in § 9, there is a diagram of order $(u/d)^2$ which contributes to $F(qjj')$ and therefore to the shift of the peaks, and which involves an intermediate optical phonon with wave vector zero or $2\pi\tau$. We omit this contribution, because it vanishes for lattices with certain symmetries, for instance for Bravais lattices.